Environmental Microbiome

RESEARCH Open Access

Unveiling the hidden world: How arbuscular mycorrhizal fungi and its regulated core fungi modify the composition and metabolism of soybean rhizosphere microbiome

Minkai Yang[1,2], Yuhang Song[1,2], Hanke Ma[1,2], Zhenghua Li[1,2], Jiawei Ding[1,2], Tongming Yin[2], Kechang Niu[1], Shucun Sun[1], Jinliang Qi[1,2], Guihua Lu[1,2,3], Aliya Fazal[1,2*], Yonghua Yang[1,2*] and Zhongling Wen[1,2*]

Abstract

Background The symbiosis between arbuscular mycorrhizal fungi (AMF) and plants often stimulates plant growth, increases agricultural yield, reduces costs, thereby providing significant economic benefits. AMF can also benefit plants through affecting the rhizosphere microbial community, but the underlying mechanisms remain unclear. Using *Rhizophagus intraradices* as a model AMF species, we assessed how AMF influences the bacterial composition and functional diversity through 16 S rRNA gene sequencing and non-targeted metabolomics analysis in the rhizosphere of aluminum-sensitive soybean that were inoculated with pathogenic fungus *Nigrospora oryzae* and phosphorus-solubilizing fungus *Talaromyces verruculosus* in an acidic soil.

Results The inoculation of *R. intraradices*, *N. oryzae* and *T. verruculosus* didn't have a significant influence on the levels of soil C, N, and P, or various plant characteristics such as seed weight, crude fat and protein content. However, their inoculation affected the structure, function and nutrient dynamics of the resident bacterial community. The co-inoculation of *T. verruculosus* and *R. intraradices* increased the relative abundance of *Pseudomonas psychrotolerans*, which was capable of N-fixing and was related to cry-for-help theory (plants signal for beneficial microbes when under stress), within the rhizosphere. *R. intraradices* increased the expression of metabolic pathways associated with the synthesis of unsaturated fatty acids, which was known to enhance plant resistance under adverse environmental conditions. The inoculation of *N. oryzae* stimulated the stress response inside the soil environment by enriching the polyene macrolide antifungal antibiotic-producing bacterial genus *Streptomyces* in the root endosphere and upregulating two antibacterial activity metabolic pathways associated with steroid biosynthesis pathways in the rhizosphere. Although inoculation of pathogenic fungus *N. oryzae* enriched *Bradyrhizobium* and increased soil urease activity, it had no significant effects on biomass and N content of soybean. Lastly, the host niches exhibited

*Correspondence:
Aliya Fazal
aliyafaxal@gmail.com
Yonghua Yang
yangyh@nju.edu.cn
Zhongling Wen
wenzhongling@nju.edu.cn

Full list of author information is available at the end of the article

differences in the composition of the bacterial community, with most N-fixing bacteria accumulating in the endosphere and *Rhizobium vallis* only detected in the endosphere.

Conclusions Our findings demonstrate that intricate interactions between AMF, associated core fungi, and the soybean root-associated ecological niches co-mediate the regulation of soybean growth, the dynamics of rhizosphere soil nutrients, and the composition, function, and metabolisms of the root-associated microbiome in an acidic soil.

Highlights

- AMF *R. intraradices* improved soybean stress resistance by recruiting specific PGPR and upregulating plant resistance promotion metabolic pathway.
- The pathogenic fungus *N. oryzae* stimulated the stress response by enriching the antifungal antibiotic production bacteria and upregulating the antibacterial reaction-associated metabolic pathways.
- The utility evaluation of some microbial agents on host plants should consider their potential impact on Olsen-P content in acidic soils with limited P availability.
- The sampling compartments (i.e., host niches of the soybean rhizosphere) exerted greater influence on the assembly and shift of the bacterial community than the application of microbial agents.

Graphical Abstract

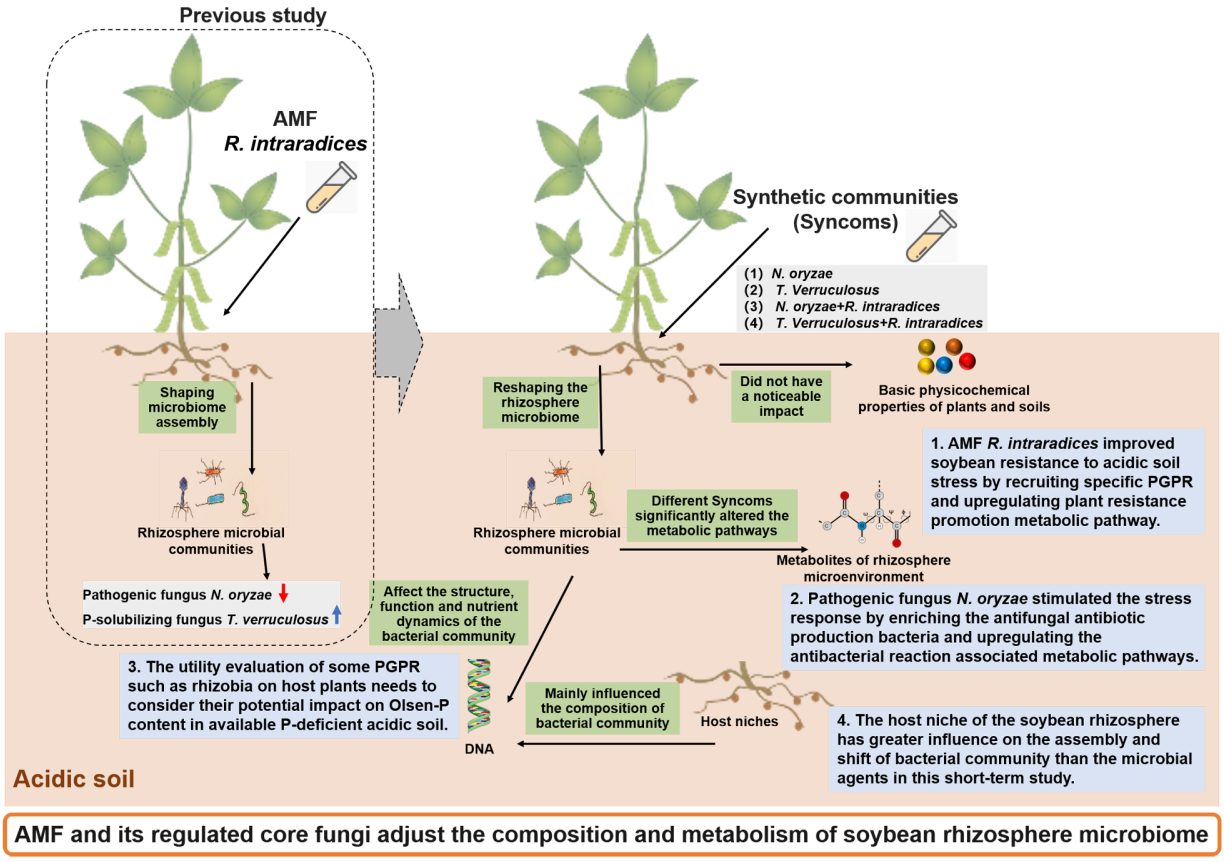

Keywords Arbuscular mycorrhizal fungi, Pathogenic fungus, Phosphorus-solubilizing fungus, Root-associated microbiome, Aluminum-sensitive soybean

Introduction

Root-soil interactions are highly complex in natural conditions, involving a multitude of active microbes [1]. Rhizosphere microorganisms are indispensable regulators of plant adaptability and productivity, which play important roles in plant water and nutrients absorption, as well as in plant resistance to biotic and abiotic stresses, and were considered as the 'second genome of plant' [2, 3]. The rhizosphere microbiome along the soil-plant continuum participates in the plant growth, nutrition, health, and

yield mainly through the interaction between plants and microbes and between microbes and microbes [4–6]. Mycorrhizal fungi and nitrogen-fixing bacteria enable plants to obtain up to 80% of their nitrogen (N) and 75% of their phosphorus (P) resources [7]. As one of the key components of the rhizosphere microbial community, arbuscular mycorrhizal fungi (AMF) directly enhance the absorption of essential nutrients such as N and P by plants, increase their resistance to biotic/abiotic stresses (e.g., drought and pathogens), and promote the colonization of N-fixing rhizobia and other plant growth promoting rhizobacteria (PGPR) in the rhizosphere of host plants [8–10]. The AMF also facilitated bacterial translocation and boosted the combination of plants with beneficial fungi and bacteria via a wide network of extraradical mycelium (ERM) [11]. The AMF and *Rhizobium* spp. have also been reported to influence the composition and abundance of other rhizosphere bacteria, and further enhance the fatty acid content, seed size, and yield of soybean grown in a semi-arid environment [12]. Other rhizosphere microbes were also closely related to plant health and nutrition, for example, root-associated microorganisms with growth-inhibitory siderophores can suppress pathogens as compared to the members with growth-promotive ones [13]. Some phosphorus solubilizing bacteria/fungi (PSB/PSF) can also dissolve insoluble minerals and organic phosphates in soil to promoting phosphorus (P) uptake of plants [14]. Some endophytic fungi can also increase the diversity of nodular culturable endophytic bacteria due to their mycelia, which are the ideal dispersal networks for rhizobia enrichment in the legume rhizosphere soil [15, 16]. Some other non-symbiotic PGPBs can promote the absorption and utilization of nutrients by improving the root structure [17], while some specific rhizosphere microorganisms can also indirectly improve the absorption of nutrients by plants and enhance their stress resistance by changing the structure and function of functional microbial communities through the interaction between microbes and microbes [18, 19]. Thus, the rhizosphere microbiome plays an important role in plant nutrition, growth, development and environmental adaptability [5, 20].

As one of the typical soil type in tropical and subtropical regions, acidic soil occupy approximately 30%/50% of the global/potential-cultivated land area [21]. Crop growth is inhibited in acid soils due to low pH value, low bio-available P and high aluminum (Al) toxicity. High levels of Al^{3+} in soil can reduce crop growth and yield by immobilizing soil P, damaging root tips, stunting roots, and inhibiting water and nutrient absorption [22, 23]. Due to the demand for the increase in crop production, some chemical fertilizers such as N fertilizers are often applied excessively, and their long-term application deteriorates soil quality, leading to further aggravation of soil acidification [24]. As a major oil and protein crop globally, soybean is also used as 'pioneer crop' to improve acidic soils because of N-fixing of its symbiotic rhizobia. The exudates of soybean, such as some organic acids like citric acid and malic acid, were found to chelate Al and closely related to the tolerance of soybean to acidic soil [25], and their root exudates had a notable impact on soil microscale environments and the composition of root-associated bacteria community [26, 27]. However, its productivity is also significantly hampered by Al stress and low available P due to the major soybean-producing regions are predominantly located in regions with acidic soils [28–30]. Moreover, nutrient-poor or extreme environments, such as acidic soils, can severely affect the composition and function of root-associated microbiomes. For instance, acidic soil inhibits soil respiration and nitrification, and influences microbial degradation of organic C and soil enzyme activity, and thereby suppresses the microbial-mediated nutrient cycles, which affects plant growth indirectly [31]. The interactions between plants and microorganisms were also directly affected by acidic soil. For example, acidic soil was reported to inhibit the signal exchange between legumes and rhizobia, reduces the process of rhizobia infecting root hairs, interferes nodulation and ultimately influences N-fixing [30]. In summary, it was urgent for us to alleviate the stress of acidic soil on plants and microorganisms through crop improvement and microbial inoculation.

Crop diversity has been successfully exploited for genetic improvement in modern breeding, which significantly contributes to yield and quality improvement in adverse environment and practical agricultural production, and produces satisfactory economic and social benefits for a long time [32, 33]. Nowadays, the application of composite microorganism agents increasingly becomes a promising new approach for crop growth promotion and soil improvement [34–36]. The synthetic communities (SynComs) constructed by soybean root associated functional microorganisms can significantly promote soybean N and P acquisition and ultimately soybean yield (up to 36.1%) [37]. The SynComs isolated from alkaline soil can regulate the growth of rhizobia specifically, and alleviated the impact of salt alkali stress on rhizobia nodulation and its colonization in nodules [38]. Special SynComs including bacteria and fungi helped soybeans resist Al toxicity by enriching plant growth promoting microorganisms [39]. Recent study indicated that the addition of AMF *Rhizophagus intraradices* agent promoted soybean biomass and increased plant C and N content by recruiting specific PGPR, thereby enhancing soybean tolerance to acidic soil in a host dependent manner [40]. Moreover, AMF *R. intraradices* were surprisingly found to reduce the abundance of pathogenic fungus *Nigrospora oryzae* while enriched P-solubilizing fungus *Talaromyces*

verruculosus in the rhizosphere soil [40]. As a P-soluble microorganisms, *T. verruculosus* is a beneficial endophytic fungus, which can improve the utilization rate of insoluble phosphorus, promote plant growth and improve plant stress resistance [41]. However, how the AMF *R. intraradices* and its regulated core fungi *N. oryzae* and *T. verruculosus* reshapes root-associated microbial community, alters soil N and P nutrient cycling and ultimately enhances soybean tolerance to acidic soil remains to be clarified.

To address these issues, an Al-sensitive soybean was used to evaluate the alterations in the nutrient dynamics, the root-associated microbes, and the soil metabolism spectrum in response to the inoculation of the AMF and its regulated fungi. Our overall hypothesis was that the inoculation of SynComs would alter the metabolism and composition of root-associated bacterial community and soil nutrient dynamics by reshaping specific functional microbiota. We anticipate that host niches along the soil-plant continuum would determine the differentiation of root-associated bacterial community following SynComs application by enriching/reducing special functional plant-growth promoting or pathogenic microorganism under environmental stress.

Materials and methods

Plant, strain and soil materials

Seeds of Bendi 2 (Al-sensitive, BD2) genotype were used as model soybean plants in the present study. The AMF strain, *Rhizophagus intraradices* (national microbial resources platform number: 1511C0001BGCAM0062, Ri) was purchased from Beijing Academy of Agriculture and Forestry Sciences (Beijing, China). The *Nigrospora oryzae* (CGMCC: 3.13798, No) and *Talaromyces verruculosus* (CGMCC: 3.5693, Tv) were purchased from the China General Microbiological Culture Collection Center (Beijing, China). The acidic soil was collected from the Ecological Experimental Station of Red Soil, Chinese Academy of Sciences (Yingtan, Jiangxi, China) (28.208° N, 116.937° E) and was diluted with sterilized sand at V(soil): V(sand) = 4:1, which with a water holding capacity of 29.3% and a pH of 4.54 (±0.21) [40].

Planting and sampling methods

The healthy soybean seeds were first surface-disinfected 16 h with chlorine (100 mL 10% NaClO + 4 mL 12 mol/L HCl), and washed 5 times with sterile water. Then the seeds were sterilized 30 s with 70% ethanol, 5 min with 2.5% sodium hypochlorite, followed by washing 5 times with sterile water again. The rhizobox was developed and improved by our laboratory (patent number CN102175487) with a length*width*height of 20 cm*15 cm*20 cm. Approximately 3.6 kg of acidic soil was placed in each rhizosbox. Soybeans were planted in the central compartment of the rhizosbox, which was separated with the two-side compartments with two layers of nylon mesh, to prevent roots from growing into the compartments on both sides [26, 40]. Then the AMF strain *R. intraradices* (10 g mixed culture powder in each rhizobox) was added to approximately 2 cm below the surface of soil before planting. Then 50 mL *N. oryzae* (cultured in Potato Dextrose Agar (PDA) medium) and *T. verruculosus* (cultured in Malt Extract Agar (MEA) medium) were resuspended in PBS, and 20 mL suspension was applied on the day 20 and 30 after planting. Original soil was unsterilized to maintain 'natural' with its native microbiota. The rhizoboxes was located in Nanjing University, Nanjing, China (32.125 N, 118.965 E). Each of the four treatments (in inoculation of No, Tv, No + Ri and Tv + Ri, respectively) had five biological replicates by using total 20 rhizoboxes. Soil samples were collected from two rhizosphere host niches from the outside to the interior of the roots, as well as two sampling stages. The experimental plant and soil were collected at the flowering stage (R2 stage, 59 days after planting) and maturing stage (R8 stage, 104 days after planting). The soils and roots materials were immediately placed in plastic bags with pre-freezing by using chemical ice packs after sampling [26, 40]. Two sampling compartments (i.e., two host niches) were collected, namely rhizosphere soil (Rh) and root endosphere (Rt). Rh samples were the soil tightly adhered to the root surface, which were collected by brushing off with phosphate buffered saline (PBS). The roots were further washed with PBS twice and placed in a 15 ml tube with 5 ml PBS (maximum at 6 ml). Then the tubes were sonicated for 20 cycles consisting of 30 s pulses and breaks of 30 s (Bioruptor Pico), centrifuged at 4000 × g for 2 min, followed by washing with PBS once more, and then the Rt samples were collected by grinding with liquid nitrogen [40]. The Rh and Rt samples for DNA extraction and metabolomics analysis were stored at -80 °C [26, 40].

Part of Rh samples were pre-treated by being air-dried and filtering through a 50 μm mesh sieve and stored at 4 °C for the detection of soil element contents and soil enzyme activities. The activities of six soil enzyme [i.e., nitrate reductase (S-NR, EC 1.7.99.4), nitrite reductase (S-NiR, EC 1.7.99.3), urease (S-UE, EC 3.5.1.5), sucrase (S-SC, EC 3.2.1.26), acid phosphatase (S-ACP, EC 3.1.3.2) and alkaline phosphatase (S-AKP/ALP, EC 3.1.3.1)], which involved in the carbon, nitrogen and phosphorus cycle, were measured according to the detailed instructions in kits (Solarbio Science & Technology Co., Ltd, Beijing, China) [40]. The other physicochemical properties of plants (e.g., plant height, plant fresh weight, 100-seed weight, crude fat (Soxhlet method) and crude protein content (Kjeldahl method) of seed) were also measured in the study [42].

DNA extraction, DNA amplicon sequencing and analysis

The Rh and Rt samples for DNA extraction analysis were first stored at -80 °C. Approximately 0.30 g of rhizosphere soil and 0.40 g root powder were used for DNA extraction via the DNeasyPowerSoil Pro Kit (QIAGEN, Hilden, Germany) after ground by a tissue grinder (Grinder-48, Gallop technology, Chengke Instrument Co., Ltd, Shanghai, China) at 60 HZ for 600 Sects. [26, 40]. The extracted DNA samples were verified with a Qubit Fluorometer (Invitrogen, Carlsbad, USA) to ensure more than 10 ng/μl [43]. The primers of the amplicons of V3-V4 hypervariable region of the 16 S rRNA gene (~468 bp) was 338 F/806R, and sequencing was performed on an Illumina NovaSeq 6000 with two paired-end read cycles of 250 bases each by OE Biotech. Co., Ltd (Shanghai, China) [40, 44]. The accession number of total 40 clean sequencing data in NCBI Sequence Read Archive database is SRP424056.

Raw sequencing data were in FASTQ format. Paired-end reads were then preprocessed using Trimmomatic software (version 0.35) and paired-end reads were assembled using FLASH software (version 1.2.11) [45, 46]. Obtain the clean tags sequence by using the split_ibraries (version 1.8.0) software in QIIME [47]. Use UCHIME (version 2.4.2) software to remove chimeras from clean tags and obtain valid tags [48]. Clean reads were subjected to primer sequences removal and clustering to generate operational taxonomic units (OTUs) using Vsearch software (version 2.4.2) with a 97% similarity cutoff [49]. The numbers of clean tags ranged from 70,817 to 74,073, and valid tags ranged from 46,980 to 64,659 with the average length between 407.09 and 415.6 bp. The number of OTUs in each sample were range from 1107 to 4204. Data was analyzed by using databases silva138/16s (http://www.arb-silva.de). Three indices, Chao1, Shannon, and Good's coverage were used to reflect the richness, diversity and coverage of microbial communities in the analysis alpha diversity, and the principal coordinate analysis (PCoA) based on Bray-Curtis distance was used to evaluate the species complexity in beta diversity [50, 51]. The functional genes analysis was conducted via the software PICRUSt. All the bioinformatic analyses were performed on OECloud platform (https://cloud.majorbio.com).

Non-targeted metabolomics analysis

The Rh samples for metabolomics analysis was first stored at -80 °C. All chemicals and solvents were analytical or HPLC grade. For the Gas Chromatograph-Mass Spectrometer (GC-MS), 500 mg soil sample was combined with 1 mL of methanol-water (V methanol: V water = 1:1) solution, which supplemented with 2 μg/mL L-2-chlorophenylalanine. The sample was ground at 60 HZ for 2 min after being placed at -40 ℃ for 2 min, then transferred to a centrifuge tube, followed by a 30 min ultrasonic in ice-water bath. Transferred the homogenized sample to a clean 15 mL centrifuge tube, followed by transferring tube wall residue twice by using a 1 mL methanol: water solution. About 1.2 mL supernatant was freeze-dried in a clean centrifuge tube after being centrifuged for 10 min (7700 rpm, 4 ℃). Then resuspended in 300 μL methanol-water, vortex for 1 min, ultrasonic for 3 min and centrifuged for 10 min (12,000 rpm, 4 ℃). About 150 μL supernatant was prepared for GC-MS analysis. A 30 m x 0.25 mm x 0.25 μm HP-5MS fused-silica capillary column (Agilent J & W Scientific, Folsom, CA, USA) was utilized to separate the derivatives. The injector temperature was maintained at 260 ℃. The program contained 60 ℃ for 0.5 min, ramped to 210 ℃ at a rate of 8 ℃/min, to 270 ℃ at a rate of 15 ℃/min, to 305 ℃ at a rate of 20 ℃/min, and finally held at 305 ℃ for 5 min. The temperature of the MS quadrupole and ion source (electron impact) was set to 150 ℃ and 230 ℃, respectively. The collision energy was 70 eV. Mass data was acquired in a full-scan mode (50–500 m/z) [52–54]. The obtained GC/MS raw data in .D format were transferred to .abf format via software Analysis Base File Converter for quick retrieval of data. All peak signal intensities were segmented, normalized, and redundancy removal and peak merging were conducted to obtain the data matrix.

For the Liquid Chromatograph-Mass Spectrometer (LC-MS), 500 mg soil sample was combined with 1 mL of 1 mL methanol water. Pre-cooling at -40 ℃ for 2 min and grinding with a grinder (60 Hz, 2 min). Use 1 mL methanol water to transfer the homogenized sample and repeat the above operation once. Centrifuge for 10 min (7700 rpm, 4 ℃) and 1.2 mL of supernatant was dried in a clean centrifuge tube in a freeze concentration centrifugal dryer. Use 300 μL methanol water (V: V = 1:4, containing L-2-chlorophenylalanine, 2 μg/mL) re-solution, vortex for 1 min, ultrasonic for 3 min, and stand at 40 ℃ for 30 min. After centrifugation for 10 min (12000 rpm, 4 ℃), a 150 μL volume of the supernatant was used for LC-MS analysis. The instrument information, program, and protocol followed the descriptions of Lai et al. and Yang et al. [55, 56]. The original LC-MS data was normalized by software Progenesis QI V2.3 (Nonlinear, Dynamics, Newcastle, UK) and the positive and negative ion data were combined to data matrix.

The overall distribution among the samples and the distinction of the metabolites between groups (containing both GC-MS and LC-MS) were observed by using partial least-squares-discriminant analysis (PLS-DA) and principal component analysis (PCA). Bioinformatic analysis was performed using the OECloud tools at https://cloud.oebiotech.com. Differential metabolites (p-values < 0.05) were selected with variable importance of projection (VIP) values greater than 1.0. All the raw data of

metabolomics along with their detailed descriptions were listed in project MTBLS7299 at database MetaboLights [57].

Statistical analyses

The statistical analyses of physicochemical properties of soils and plants, enzyme activities, alpha diversity indices and differential composition of the bacterial taxa and metabolites were evaluated according to one-way ANOVA in Graphpad Prism, followed by the Tukey test (*$p<0.05$) [40, 58]. The PERMANOVA analysis (Adonis) and similarities (ANOSIM) were performed by using the vegan package of R software (v3.1.3) based on the Bray-Curtis distance metric [59].

Results

Physicochemical properties of soils and plants

The radar chart mainly reflected the effects of the application of different Syncoms on the physicochemical properties of plants and soil at flowering and maturing stages. The results showed that the co-application of pathogenic fungus *N. oryzae* and AMF *R. intraradices* seemed to have improvement effects on the height and fresh weight of soybean at flowering stage (Fig. 1A), as well as the height and N content of soybean at the maturing stage (Fig. 1C). Then the addition of P-solubilizing fungus *T. verruculosus* was found to increase the C/N ratio of soybean at both flowering and maturing stages (Fig. 1AC), while the co-application of *T. verruculosus* and *R. intraradices* promoted the P contents of soybean at maturing (Fig. 1C). As shown in Table 1, the results of statistical analyses showed that the addition of *T. verruculosus* significantly decreased the plant height, the N and P

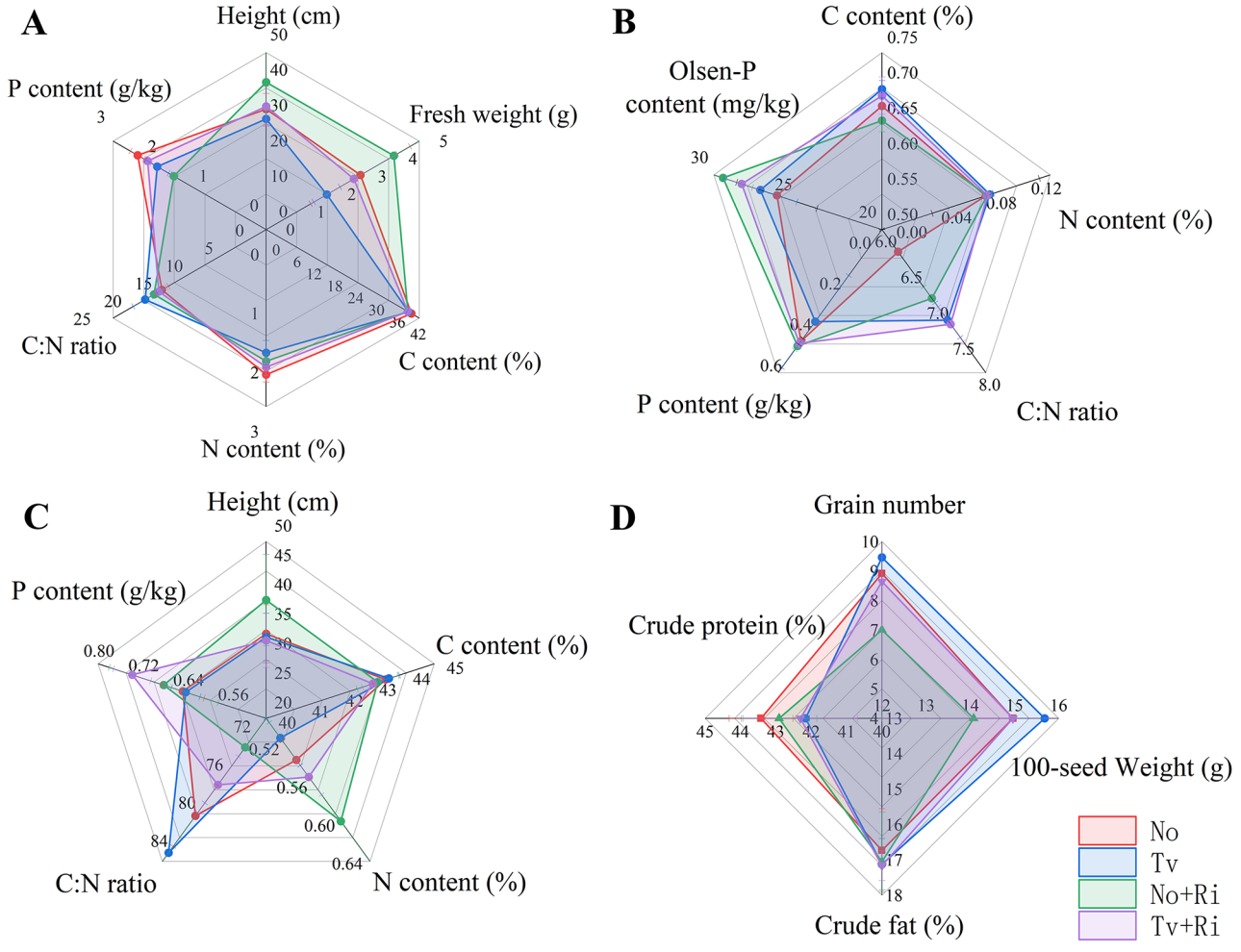

Fig. 1 The basic physicochemical properties of plants and soils. (**A**) The radar map of six physicochemical properties of plant at flowering stage. (**B**) The radar map of five physicochemical properties of soil at flowering stage. (**C**) The radar map of five physicochemical properties of plant at maturing stage. (**D**) The radar map of three physicochemical properties of seed at maturing stage. No, Tv and Ri represent inoculation of *Nigrospora oryzae*, *Talaromyces verruculosus* and *Rhizophagus intraradices*, respectively

Table 1 Basic physicochemical properties of plants and soils

Sampling stages	Compartments	Traits	*No*	*Tv*	*No + Ri*	*Tv + Ri*
			(Mean ± SD)			
Flowering stage	Plant	Height (cm)	34.02 ± 4.44 ^{ab}	31.26 ± 2.01 ^{b}	41.62 ± 8.47 ^{a}	34.8 ± 5.60 ^{ab}
		Fresh weight (g)	3.08 ± 1.62	1.98 ± 0.43	4.47 ± 2.19	2.87 ± 1.42
		C content (%)	41.76 ± 0.36	40.95 ± 0.39	40.75 ± 0.86	40.74 ± 0.62
		N content (%)	2.46 ± 0.12 ^{a}	2.01 ± 0.21 ^{b}	2.23 ± 0.12 ^{ab}	2.33 ± 0.15 ^{ab}
		C: N ratio	17.02 ± 1.04 ^{b}	19.77 ± 1.94 ^{a}	18.32 ± 1.27 ^{ab}	17.53 ± 1.26 ^{ab}
		P content (g/kg)	2.52 ± 0.14 ^{a}	2.14 ± 0.22 ^{b}	1.81 ± 0.06 ^{c}	2.32 ± 0.07 ^{ab}
	Soil	C content (%)	0.68 ± 0.41	0.70 ± 0.01	0.65 ± 0.02	0.69 ± 0.03
		N content (%)	0.09 ± 0.05	0.10 ± 0.00	0.09 ± 0.00	0.09 ± 0.00
		C: N ratio	6.31 ± 2.21	7.27 ± 0.24	6.96 ± 0.16	7.32 ± 0.24
		P content (g/kg)	0.55 ± 0.01	0.45 ± 0.23	0.57 ± 0.02	0.56 ± 0.02
		Olsen-P content (mg/kg)	26.25 ± 2.36	27.24 ± 2.18	29.45 ± 1.75	28.34 ± 0.96
Maturing stage	Plant	Height (cm)	34.34 ± 4.93 ^{b}	33.79 ± 4.03 ^{b}	40.06 ± 7.75 ^{a}	33.21 ± 4.62 ^{b}
		C content (%)	43.56 ± 0.37	43.65 ± 0.31	43.32 ± 0.61	43.17 ± 0.30
		N content (%)	0.54 ± 0.02	0.52 ± 0.03	0.61 ± 0.10	0.56 ± 0.02
		C: N ratio	80.22 ± 3.21	84.09 ± 5.24	73.03 ± 13.16	76.97 ± 2.96
		P content (g/kg)	0.65 ± 0.04	0.64 ± 0.03	0.68 ± 0.10	0.74 ± 0.03
	Seed	100-seed Weight (g)	14.97 ± 3.45	15.69 ± 3.27	14.08 ± 2.73	14.96 ± 4.01
		Crude fat (%)	16.73 ± 1.18	17.12 ± 0.73	17.05 ± 1.41	17.17 ± 0.42
		Crude protein (%)	43.42 ± 0.90	42.16 ± 0.17	42.91 ± 1.07	43.31 ± 1.62

SD stands for standard deviation. Statistical analysis was performed by using one-way ANOVA. The values with different superscript letters indicate the significant difference ($p < 0.05$) between groups. No, Tv and Ri represent *Nigrospora oryzae*, *Talaromyces verruculosus* and *Rhizophagus intraradices*, respectively. Rh and Rt represent rhizosphere soil and root endosphere

contents of soybean at the flowering stage. Although the co-application of *N. oryzae* and *R. intraradices* decreased the P contents of soybean at flowering, they significantly increased the plant height at both flowering and maturing stages (Table 1). However, the addition of all fungal agents had no obvious impacts on C, N, P contents or available P (Olsen-P) content of soil, as were the hundred seed weight, crude fat and crude protein content of seed (Fig. 1; Table 1). The activities of sucrase, nitrate and nitrite reductase, acid and alkaline phosphatase in the rhizosphere soil were unaffected by the application of *N. oryzae*, *T. verruculosus* and *R. intraradices*, whereas only the activity of urease under co-application of *N. oryzae* and *R. intraradices* was higher than under co-application of *T. verruculosus* and *R. intraradices* (Fig. 2).

Alpha and Beta diversity of soybean rhizosphere bacterial community

The rarefaction curves of the observed OTU numbers of samples indicated that the sequencing depth and the OTU coverage of the samples included sufficient detectable species in bacterial communities and captured the diversity of bacterial communities (Figure S1). The addition of different SynComs (i.e., *N. oryzae*, *T. verruculosus* and *R. intraradices*) had no significant impacts on the richness and abundance of bacterial community in both the rhizosphere soil and root endosphere (Fig. 3ABC). However, the values of Chao1 and Shannon indices in the root endosphere were lower than those in the rhizosphere soil, while the Good's coverage was higher in the root endosphere than rhizosphere soil (Fig. 3 ABC). Thus, the selection effect of soybean roots reduced the richness and diversity and increased the community coverage of root-associated microbiome.

The PCoA charts revealed that the rhizosphere bacterial community was not dominated by the SynComs treatments, but clearly segregated by two different sampling compartments (i.e., rhizosphere soil and root endosphere) (Fig. 3DEF). Then the ANOSIM and Adonis analyses showed that there exhibited no difference between the groups with and without the application of *R. intraradices* (Table 2). Statistical analysis also indicated substantial variations between *N. oryzae* and *T. verruculosus* treatments, and host niches had an appreciable effect on the composition of soybean rhizosphere microbiome (p-value < 0.05) (Table 2).

Comparison of the compositions and functions of rhizosphere bacterial community

The comparison of the top abundant 20 phyla of the bacterial community revealed that the addition of SynComs exhibited no significant impact on the compositions of soybean rhizosphere microbiome at phylum level (Figure S2AB). In addition, when making comparison between different sampling compartments, the abundances of Chloroflexi, Acidobacteriota, Myxococcota and Gemmatimonadetes were significantly lower in the root endosphere than in the rhizosphere soil (Figure S2AB).

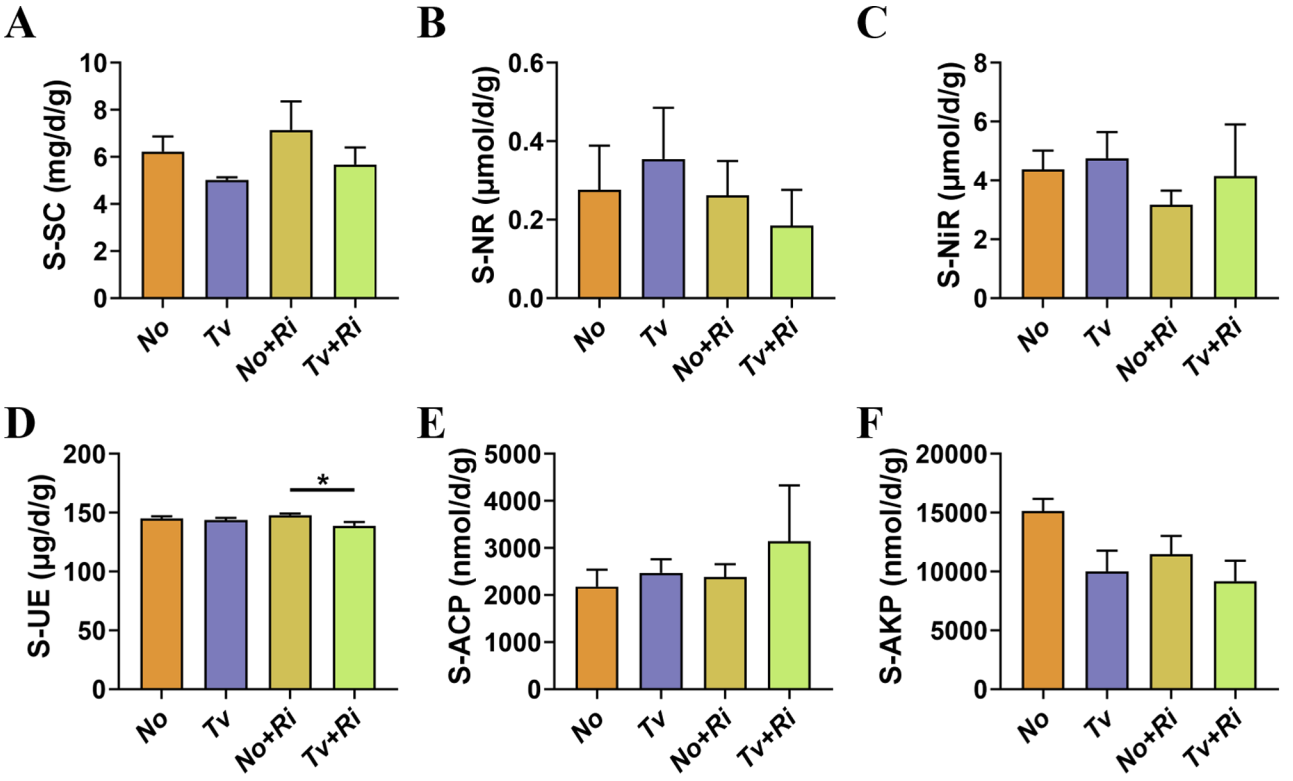

Fig. 2 The activities of six key enzymes involved in the carbon, nitrogen and phosphorus cycle in the rhizosphere soil. S-SC (**A**), S-NR (**B**), S-NiR (**C**), S-UE (**D**), S-ACP (**E**) and S-AKP (**F**) represent sucrase (EC 3.2.1.26), nitrate reductase (EC 1.7.99.4), nitrite reductase (EC 1.7.99.3), urease (EC 3.5.1.5), acid phosphatase (EC 3.1.3.2) and alkaline phosphatase (EC 3.1.3.1), respectively. No, Tv and Ri represent inoculation of *Nigrospora oryzae*, *Talaromyces verruculosus* and *Rhizophagus intraradices*, respectively. The error bars represent the standard deviation and the asterisk (*$p < 0.05$) indicates a significant difference by the Tukey test according to one-way ANOVA

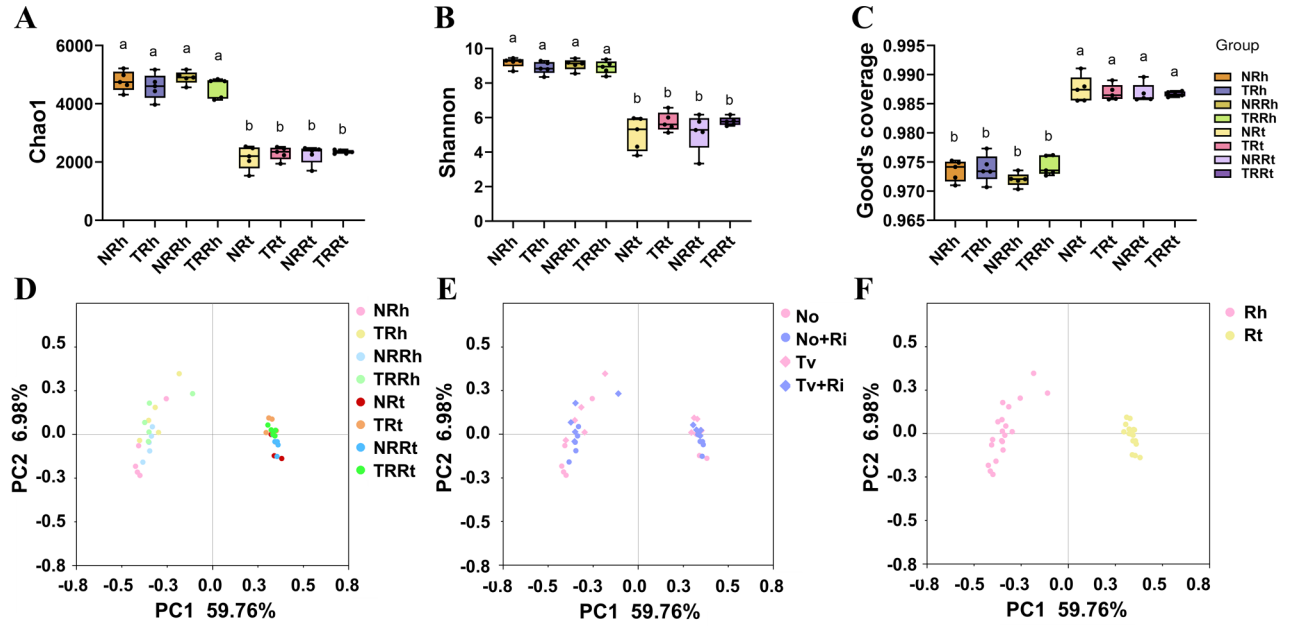

Fig. 3 The alpha and beta diversity of root-associated bacterial community ($n = 5$). The boxplot of alpha diversity was analyzed through Chao1 (**A**), Shannon (**B**) and Good's coverage (**C**) indices. The beta diversity of all groups (**D**), treatment groups (**E**) and host niches groups (**F**) were analyzed through PCoA. N, T and R represent *Nigrospora oryzae*, *Talaromyces verruculosus* and *Rhizophagus intraradices*, respectively. Rh and Rt represent rhizosphere soil and root endosphere, respectively. Other treatment details were shown in Fig. 2. Different superscript letters indicate the significant difference ($p < 0.05$) between groups by the Tukey test according to one-way ANOVA

Table 2 Statistical analyses of bacterial community structure of rhizosphere soil and root endosphere

Group vs. Group	Adonis		ANOSIM	
	R^2	*p*-value	Statistic	*p*-value
NRh vs. **T**Rh	0.21997	**0.042**	0.26	**0.039**
NRh vs. NRRh	0.09413	0.513	0.044	0.253
TRh vs. TRRh	0.09247	0.692	-0.10799	0.885
NRRh vs. TRRh	0.14208	0.123	0.13599	0.082
NRt vs. **T**Rt	0.28233	**0.01**	0.476	**0.007**
NRt vs. NRRt	0.04275	0.977	-0.128	0.875
TRt vs. TRRt	0.08571	0.619	-0.11199	0.791
NRRt vs. **TR**Rt	0.216	**0.044**	0.31599	**0.047**
N**Rh** vs. N**Rt**	0.70163	**0.008**	1	**0.007**
T**Rh** vs. T**Rt**	0.62489	**0.007**	1	**0.007**
NR**Rh** vs. NR**Rt**	0.70239	**0.012**	1	**0.01**
TR**Rh** vs. TR**Rt**	0.60322	**0.01**	0.99199	**0.015**
(N + NR) Rh vs. **(T + TR)** Rh	0.13492	**0.002**	0.26044	**0.001**
(N + NR) Rt vs. **(T + TR)** Rt	0.22159	**0.001**	0.46444	**0.001**
(N + T) Rh vs. (NR + TR) Rh	0.04051	0.734	-0.03844	0.813
(N + T) Rt vs. (NR + TR) Rt	0.02731	0.891	-0.07433	0.893
(N + NR) **Rh** vs. (N + NR) **Rt**	0.68181	**0.001**	1	**0.001**
(T + TR) **Rh** vs. (T + TR) **Rt**	0.5845	**0.001**	0.99822	**0.001**
(N + T) **Rh** vs. (N + T) **Rt**	0.59094	**0.001**	0.99888	**0.001**
(NR + TR) **Rh** vs. (NR + TR) **Rt**	0.60183	**0.001**	0.99955	**0.001**
Rh vs. **Rt**	0.58491	**0.001**	0.99905	**0.001**

N, T and R represent *Nigrospora oryzae*, *Talaromyces verruculosus* and *Rhizophagus intraradices*, respectively. Rh and Rt represent rhizosphere soil and root endosphere. The *p*-values with significant difference between groups, along with the difference parameters in the statistical group with differences were marked in bold

Moreover, the relative abundance of *Sphingomonas* was lower in the root endosphere, whereas *Bradyrhizobium*, *Streptomyces*, *Thermosporothrix* and *Allorhizobium-Neorhizobium-Pararhizobium-Rhizobium* were higher in the root endosphere than in the rhizosphere soil at genus level (Figure S2CD). The genus *Burkholderia-Caballeronia-Paraburkholderia* had no difference in abundance between two host niches according to one-way ANOVA, even though it seemed to be enriched in the rhizosphere soil (Figure S2CD). When making comparison between different SynComs application groups, the genus *Bradyrhizobium* and *Streptomyces* were found to be enriched under *N. oryzae* groups than *T. verruculosus* groups in the root endosphere according to one-way ANOVA (Figure S2CD). The genus *Burkholderia-Caballeronia-Paraburkholderia* and the species *Trinickia symbiotica* (which belongs to *Burkholderia* sensu lato), seemed abundant in *T. verruculosus* treatment than in *N. oryzae* treatment; however, no significant difference in statistical analysis was found between different treatments (Figure S2C-F).

Then the comparison of the abundance of all classified N-fixing bacteria at genus level showed that the application of SynComs exhibited no significant effects on most free-living, associative and symbiotic N-fixing bacteria (Fig. 4AB). However, *N. oryzae* increased the abundance of *Bradyrhizobium* in root endosphere (Fig. 4B and Figure S2CD). Additionally, although the SynComs had no significant influence on 3 of 4 classified bacteria species that were closely related to N-fixing, the co-application of *T. verruculosus* and *R. intraradices* was found to enrich *Pseudomonas psychrotolerans* in the rhizosphere soil (Fig. 4C). Lastly, the *Rhizobium vallis* was detected exclusively in the root endosphere of soybean (Fig. 4C).

The analysis of predicted functional genes by PICRUSt implied that, different SynComs treatments exhibited no significant impact on the overall composition and abundance of functional genes (Figure S3A). The amino acid transport and metabolism being the most prevalent functional genes, followed by transcription and signal transduction mechanisms (Figure S3A). Seven COG functional classifications were found to be closely related to N-fixing, three of them, COG0347 (nitrogen regulatory protein PII), COG1348 (nitrogenase subunit NifH) and COG2710 (nitrogenase molybdenum-iron protein), were shown to be enriched in the root endosphere than in rhizosphere soil (Figure S3B). Six COG functional classifications were identified directly related to acid/alkaline phosphatase, four of them, COG0496 (acid phosphatase), COG1368 (alkaline phosphatase superfamily), COG1785 (alkaline phosphatase), and COG3540 (phosphodiesterase/alkaline phosphatase D), were also enriched in the root endosphere (Figure S3B). Lastly, the COG2710 and COG3540 were abundant in the endosphere under the *N. oryzae* addition as compared to *T. verruculosus* addition (Figure S3BC).

Metabolic response of the application of synthetic communities

The GC-MS non-targeted metabolomics analysis identified a total of 177 metabolites in four groups of rhizosphere soil samples. The PCA and PLS-DA analyses indicated that the soil metabolism spectrum changed significantly in response to SynComs application according to the obvious differences in the aggregation positions of the different treatment groups (Figure S4). The metabolites responsible for the separation between different groups were screened by VIP scores (>1), and the number of identified differentially expressed metabolites (DEMs) was shown in the volcano plots and heatmap plots (Figure S5). A total of 18 DEMs were found in the AMF addition groups (w-Ri, with Ri inoculation, i.e., No + Ri and Tv + Ri groups) as compared to non-AMF addition groups (wo-Ri, without Ri inoculation, i.e., No and Tv groups), 12 DEMs such as hydroquinone, glyceric acid, behenic acid, butanedioic acid, arachidic acid and tetracosanoic acid were upregulated, while 6 DEMs such as ciliatine, aconitic acid, beta-sitosterol and oleic acid were downregulated (Figure S5C). Additionally, when making comparison with *N. oryzae* application group,

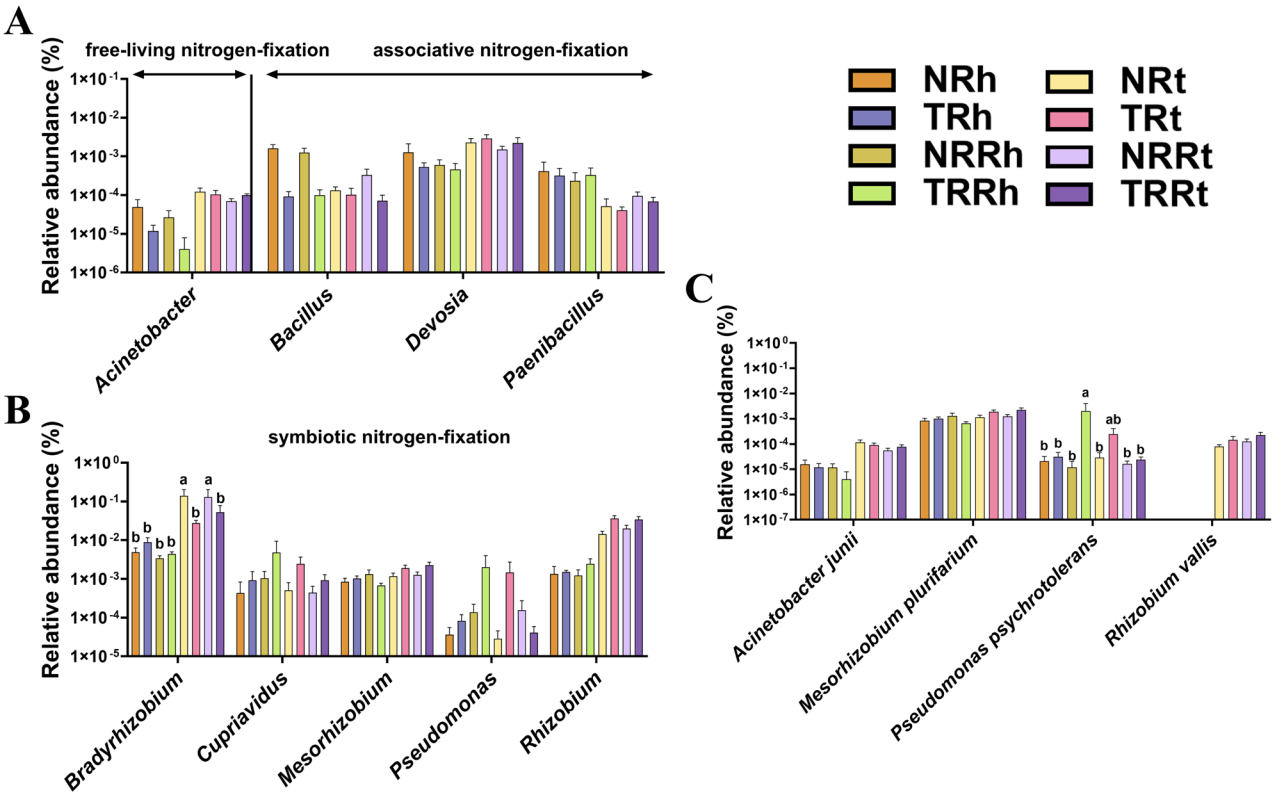

Fig. 4 The relative abundance of major nitrogen-fixing bacteria phyla and species in soybean root-associated bacterial community. (**A**) The relative abundance of major free-living and associative nitrogen-fixing bacteria at genus level. (**B**) The relative abundance of major symbiotic nitrogen-fixing bacteria at genus level. (**C**) The abundance of nitrogen-fixing bacteria at species level. Genera *Rhizobium* represent *Allorhizobium-Neorhizobium-Pararhizobium-Rhizobium* in database. N, T, NR and TR represent *N. oryzae*, *T. verruculosus*, *N. oryzae* + *R. intraradices*, and *T. verruculosus* + *R. intraradices* respectively. Rh and Rt represent rhizosphere soil and root endosphere

the *T. verruculosus* application group had 1 upregulated metabolite 1,5-anhydroglucitol and 11 downregulated metabolites such as beta-hydroxymyristic acid, sucrose, and malic acid (Figure S5D).

The mechanism of metabolites changes under different SynComs additions was likely a result of reprogramming of multiple metabolic pathways [60]. Results of pathway enrichment analyses were shown in Figure S6 ($p<0.05$). The application of *R. intraradices* significantly enriched five metabolic pathways, for example, biosynthesis of unsaturated fatty acids, glycerolipid metabolism, and glyoxylate and dicarboxylate metabolism ($p<0.01$) (Figure S6A). In addition, the pathway analysis of *T. verruculosus* group revealed the significant enrichment of several metabolic pathways, including taste transduction, steroid biosynthesis, renal cell carcinoma and bacterial chemotaxis pathways, as compared to *N. oryzae* group (Figure S6B). The comparison of the abundance of metabolites involved in key metabolic pathways showed that, three DEMs (arachidic acid, behenic acid, and tetracosanoic acid) belonged to biosynthesis of unsaturated fatty acids were enriched, while the oleic acid was depleted in AMF addition groups as compared to non-AMF addition groups (Fig. 5A and Figure S5C). As shown in Fig. 5A, the *T. verruculosus* group had lower oleic acid abundance as compared to *N. oryzae* group. The AMF addition groups had a higher abundance of glucose-1-phosphate and glyceric acid which were involved in glycerolipid metabolism pathway, than the non-AMF addition groups (Figure S5C); however, there exhibited no difference between the single-variable comparison groups (Fig. 5B). Two DEMs involved in steroid biosynthesis pathway, beta-sitosterol and stigmasterol, were downregulated under *T. verruculosus* treatments when making comparison to *N. oryzae* addition groups (Figure S5D), and only beta-sitosterol in was found to have lower abundance in *T. verruculosus* group as compared to *N. oryzae* group (Fig. 5C). Lastly, the butanedioic acid was abundant in *R. intraradices* group and malic acid was abundant in *N. oryzae* group, and these two DEMs directly involved in the citrate cycle (TCA cycle) (Fig. 5D and Figure S5CD).

The LC-MS analysis then identified a total of 4475 metabolites. Compared with GC-MS, the LC-MS analysis displayed about 25-folds identified metabolites, and approximately 10-folds identified DEMs (Table S1). Although the GC-MS analysis found more upregulated

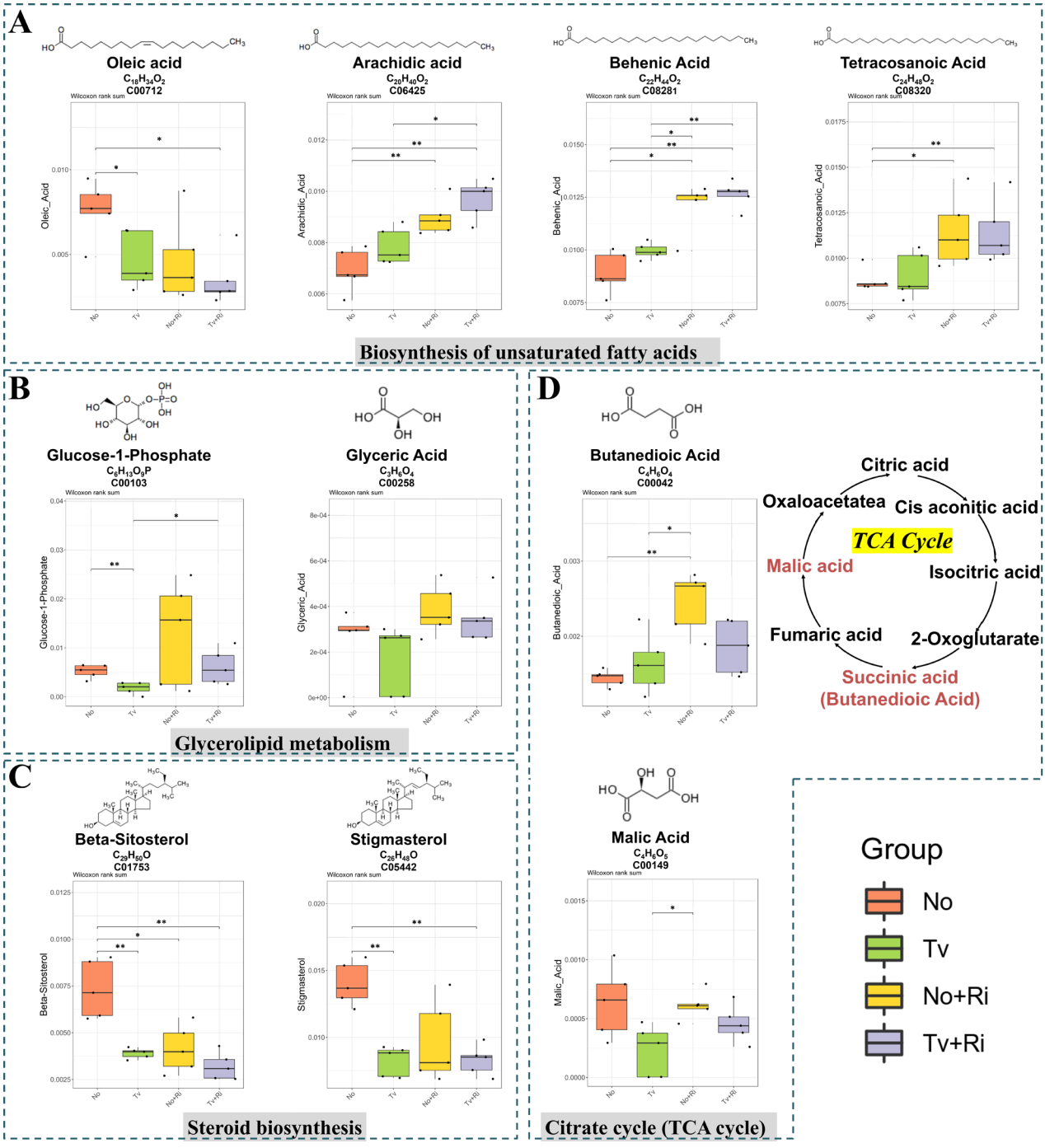

Fig. 5 The relative abundance of identified differential metabolites between groups ($n=5$) in key KEGG metabolic pathways. These KEGG metabolic pathways were descripted as biosynthesis of unsaturated fatty acids (**A**), glycerolipid metabolism (**B**), steroid biosynthesis (**C**) and citrate cycle/TCA cycle (**D**). No, Tv and Ri represent *Nigrospora oryzae* inoculation, *Talaromyces verruculosus* inoculation and *Rhizophagus intraradices* inoculation. Statistical assessment in box plots was performed using Wilcoxon-rank-sum test, asterisks indicate the significant difference (*$P<0.05$, **$P<0.01$) between groups. Other treatment details were shown in Fig. 2

than downregulated DEMs in the AMF addition groups, the LC-MS analysis showed an opposite result (Table S1). AMF application decreased the abundance of almost 4/5 metabolites (98/120) such as polidocanol, pentaethylene glycol and heptaethylene glycol monododecyl ether. Then the detailed comparison of the differential metabolites in the rhizosphere soil between AMF addition groups and non-AMF addition groups showed that there exhibited a positive correlation between 3-Ketosphingosine, 5'-Carboxy-gamma-chromanol

and [(2 S,4R,5R,6R,14 S,16R)-14-Hydroxy-7,11-dimethyl-6-(2-oxopyran-4-yl)-3-oxapentacyclo [8.8.0.02,4.02,7.011,16]octadecan-5-yl] acetate, while there three metabolites were negatively correlated with most other metabolites (Figure S7A). Other metabolites were positively correlated with each other (Figure S7A). The Pearson-correlation analysis indicated a positive correlation (p value < 0.05, correlation > 0.95) when analyzing the co-occurrence patterns of major metabolites (Figure S7B). Three differential metabolites, pyrimidine metabolism, ABC transporters, and pentose phosphate pathway were upregulated, while four metabolites such as valine, leucine and isoleucine biosynthesis, and propanoate metabolism pathway were downregulated in AMF addition groups than in non-AMF addition groups according to enrichment plots (p value < 0.05) (Figure S7CE).

Microbial co-occurrence network analysis

RDA analysis revealed the relationship between the environmental factors and the structure of bacterial community. As shown in Fig. 6A, the red and blue arrows represented 4 different environmental factors and 10 major bacterial genera. The results showed that the total C and N content of soil were positively correlated with some main N-fixing bacterial genera such as *Allorhizobium-Neorhizobium-Pararhizobium-Rhizobium*, meanwhile the soil C and N content were negatively correlated with available P content of soil (Fig. 6A). Then the Pearson correlation analysis of plant physicochemical properties and the 10 major bacterial genera implied that, at flowering stage, the *Acidipila* had negative correlation with total C (%) (r=-0.574, p=0.0081) and total P (g/kg) (r=-0.452, p=0.0455) of soybean, as were *Thermosporothrix* with total N (%) (r=-0.481, p=0.0319) of soybean (Fig. 6B). The total N (%) of soybean at maturing stage exhibited co-occurrence correlations with *Acidipila*

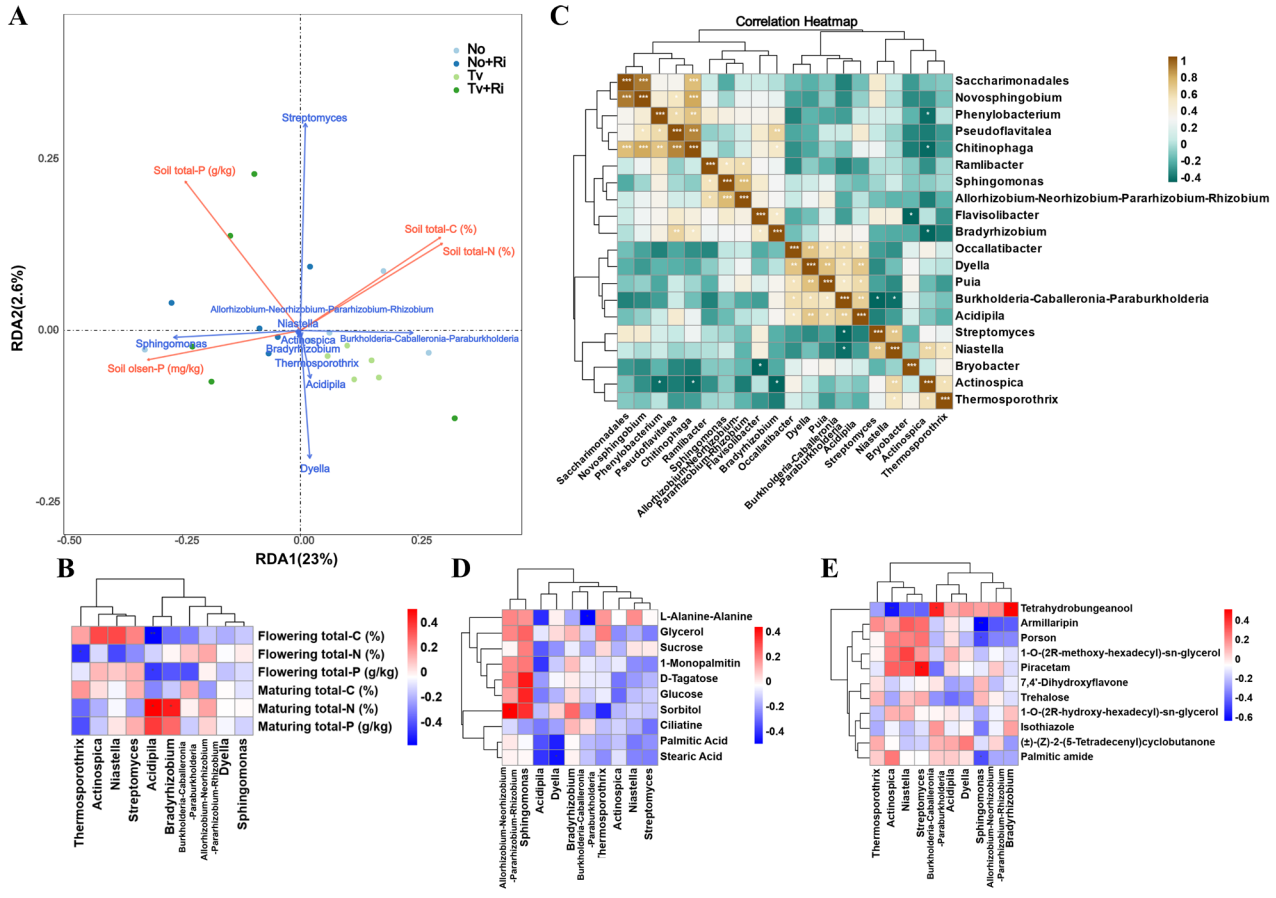

Fig. 6 Correlation analysis between plant and soil physicochemical properties, composition of rhizosphere bacterial community and rhizosphere metabolites. (**A**) RDA analysis plot of the 10 major bacterial genera in rhizosphere and 4 soil physicochemical properties. (**B**) The Pearson correlation results of 6 plant physicochemical properties and top 10 bacterial genera in rhizosphere. (**C**) The Pearson correlation results of top 20 bacterial genera associated with the rhizosphere soil of soybean. The Pearson correlation results of the 10 major bacterial genera in rhizosphere and 10 major metabolites of GC-MS (**D**) and LC-MS (**E**). Significant correlations (*P < 0.05, **P < 0.01, and ***P < 0.001) and the positive and negative correlation were shown in figures. Other treatment details were shown in Fig. 2

(r=0.520, p=0.0188) and *Bradyrhizobium* (r=0.461, p=0.0405) (Fig. 6B).

To understand the feedbacks between microorganisms that occur among soybean rhizosphere soil, the co-occurrence patterns of the 20 major bacterial genera associated with the rhizosphere soil of soybean were also analyzed (Fig. 6C). As shown in Fig. 6C, there existed significant positive correlation (r>0, p<0.05) between *Occallatibacter*, *Dyella*, *Puia*, *Burkholderia-Caballeronia-Paraburkholderia* and *Acidipila*. The *Sacchari-monadales* also had positive co-occurrence correlations with *Novosphingobium* (r=0.881, $p=2.98\times10^{-7}$) and *Chitinophaga* (r=0.686, p=0.0008) (Fig. 6C). Further analysis of the relationship between composition of soil microbiome and rhizosphere metabolites via 10 major bacterial genera and 10 major metabolites revealed that, the *Allorhizobium-Neorhizobium-Pararhizobium-Rhizobium* was found to have positive correlations with sorbitol (r=0.450, p=0.0466), *Dyella* was negatively correlated with stearic acid (r=-0.458, p=0.0422) while *Burkholderia-Caballeronia-Paraburkholderia* was negatively corelative to L-alanine-alanine (r=-0.488, p=0.0291) (Fig. 6D). The *Streptomyces* had positive correlations with piracetam (r=0.489, p=0.0286), while *Sphingomonas* was negatively correlated with porson (r=-0.458, p=0.0422), armillaripin (r=-0.624, p=0.0033) and palmitic amide (r=-0.449, p=0.0468) (Fig. 6E). The tetrahydrobungeanool were found to have positive correlations with *Burkholderia-Caballeronia-Paraburkholderia* (r=0.451, p=0.0460) and *Bradyrhizobium* (r=0.525, p=0.0175), and was negatively correlative to *Actinospica* (r=-0.582, p=0.0071) (Fig. 6E).

Discussion

Microbial inoculants modified the structure and function of rhizosphere microbiome

SynCom always represent viable, complex and stable community selected and engineered from a core microbiota [61]. Our recent study found that the abundance of pathogenic fungus *N. oryzae* and P-solubilizing fungus *T. verruculosus* was regulated by AMF *R. intraradices*. Thus, in this study, we used SynCom to represent these three artificial microbial agents above. In our study, host niches displayed differentiation of associated bacterial community following Syncoms inoculations. Both the single-strain inoculation and combined inoculations had no significant effects on bacterial alpha diversity. Endosphere had lower microbial richness (Chao1) and Shannon diversity than the rhizosphere, while higher Good's coverage than rhizosphere (Fig. 3ABC). The beta diversity using PCoA revealed that endopshere and rhizosphere niches were clearly separated following both single strain and co-inoculation (Fig. 3DEF). Moreover, taxonomic studies revealed higher abundances of Chloroflexi, Acidobacteriota, Myxococcota and Gemmatimonadetes in the rhizosphere than in the endosphere (Figure S2AB). Furthermore, the *Rhizobium vallis* was only detected in the root endosphere (Fig. 4C). A recent study suggests that the rhizosphere microbiome is divided into the environment-dominated and plant genetic-dominated components, while the physical, chemical, and biological characteristics of rhizosphere soil mainly determine the assembly of the environment-dominated microbiome (up to 96.5%) [62]. Although the bacterial community was found to exhibit significant differences mainly between two host niches, significant statistical differences were also detected between *N. oryzae* and *T. verruculosus* treatments according to the analyses of ANOSIM and Adonis (Table 2). In addition, the co-inoculation of *T. verruculosus* and *R. intraradices* was found to increase the relative abundance of a N-fixer, *Pseudomonas psychrotolerans*, in the rhizosphere (Fig. 4C). The potential P-soluble fungus *T. verruculosus* was also reported to have cellulolytic characteristic [41, 63]. *Pseudomonas* populations were one of the famous plant growth-promoting rhizobacteria (PGPR), which can promote photosynthetic capacity by improving the plant chlorophyll content [64], and are directly involved in nutrient metabolism of C, N, and P in soil [65, 66]. Therefore, inoculation with *T. verruculosus* not only improved soil P nutrition, but also had direct and indirect effects on C nutrition. Moreover, the *N. oryzae* inoculation enriched *Bradyrhizobium* and *Streptomyces* in endosphere (Figure S2CD). The famous efficient antimycotic and antiprotozoal agent, polyene macrolide antibiotic, was produced by several soil bacterial species of the genus *Streptomyces* [67, 68]. Thus, the addition of pathogenic fungi might directly stimulate the enrichment of anti-pathogenic fungal microorganisms in the soybean rhizosphere. Moreover, a new study suggested that, the carbon compounds exuded by AMF genus *Rhizophagus* were acquired by the bacterium which could mineralize organic P, while *Streptomyces* inhibited the bacteria with weak P-mineralizing ability and enhanced AMF to acquire P [69], which proved that the role of *Streptomyces* in the AMF-mediated rhizosphere microbial community needed deeper exploration. Functional classification revealed the itrogenase molybdenum-iron protein (COG2710) and phosphodiesterase/alkaline phosphatase D (COG3540) were enriched in the endosphere upon *N. oryzae* inoculation (Figure S3BC). Our findings thus suggest that fungal inoculation could modulate the interactions among bacteria residing in the host plant niches, thus affecting the structure, function and dynamics of the resident bacterial community. These results also corroborate previous findings that the microbial inoculants could alter the diversity, network stability, structure and functionality of soil and plant microbiome [70], modify metabolite-soil-microbial interactions [71],

and regulate secondary metabolites exudation and rhizosphere expansion [72].

Microbial inoculants adjusted the metabolic spectrum in the rhizosphere microenvironment

The composition of the plant-associated microbiome is influenced by various factors, including host genotype, root morphology, and root exudates [73]. In turn, changes in plant metabolic profiles caused by microbial inoculations might have an impact on the patterns of root exudation [74]. Thus, understanding the chemical characteristics of rhizosphere soil can give us insights into its effects on microbial community structure [75]. LC-MS has higher detection sensitivity and is more sensitive to trace substances, while GC-MS has better separation and detection effect and a more comprehensive database. In our investigation, the effect of single strain or co-inoculation on the assembly and shift of soil microbes could be due to their ability to modify the metabolic profile of host plant via interfering root exudation patterns. To prove this, GC-MS of rhizosphere soil samples was performed, and it was observed that AMF application upregulated DEMs which belong to biosynthesis of unsaturated fatty acids, such as arachidic acid, behenic acid, and tetracosanoic acid, as compared to non-AMF addition groups (Fig. 5A and Figure S5C). Unsaturated fatty acids are known to have a significant influence on enhancing plant resistance under adverse environmental conditions [76]. One famous plant growth promoting rhizobacteria, *Pseudomonas psychrotolerans* [77], was found to be enriched in the rhizosphere under the co-inoculation of *T. verruculosus* and *R. intraradices*, which might be co-related to the upregulation of the expression levels of biosynthesis of unsaturated fatty acids. *Pseudomonas* species in soil have been proved to be closely related to soybean stress resistance by exudating key metabolites such as purine, which also supports the previously reported cry-for-help theory [78, 79]. These findings imply that the inoculation of AMF *R. intraradices* may improve soybean resistance to acidic soil stress by modifying the chemical and microbiological composition of the soybean rhizosphere. Two DEMs involved in the steroid biosynthesis pathway, beta-sitosterol and stigmasterol, were found to have higher abundance in *N. oryzae* addition groups as compared to *T. verruculosus* treatments (Figure S5D). The steroid hormones are considered to be regulators of plant growth, development, and stress responses, and beta-sitosterol and stigmasterol are also known for their antibacterial activity [80–82]. Thus, the application of *N. oryzae* activated the antibacterial reaction in the soil microenvironment, which was also consistent with our finding in the composition of the bacterial taxa, that the polyene macrolide antibiotic production bacterial genus *Streptomyces* was abundant in endosphere under *N. oryzae* inoculation (Figure S2CD). Some metabolic pathways, such as taste transduction and renal cell carcinoma, existed significant differences between different treatments (Figure S6B), which might be closely related to protozoon such as *Caenorhabditis elegans* [83, 84]. Lastly, the LC-MS displayed about 25-fold identified metabolites and approximately 10-folds identified DEMs as compared with GC-MS, and the results of LC-MS indicated that AMF application decreased the abundance of almost 4/5 metabolites, which were also worth further study (Table S1).

The application of microbial agents needs to consider the complex interactions in the rhizosphere microenvironment

The *N. oryzae* inoculation enriched *Bradyrhizobium* in endosphere (Figure S2CD). The Pearson correlation analysis showed that the total N of soybean at maturing stage exhibited co-occurrence correlations with *Acidipila* and *Bradyrhizobium* (Fig. 6B). *Bradyrhizobium* is the dominant rhizobia in acidic soils, thus, the colonization of dominant rhizobia in acidic soil might directly increase plant N content. In addition, the co-inoculation of *N. oryzae* and *R. intraradices* significantly increased the activity of urease (Fig. 2). Through catalysing the breakdown of urea into CO_2 and NH_3, urease has an important role in the N cycle by generating accessible N for plant growth and might be a good index of soil quality [85]. However, the *N. oryzae* application was found to have no significant effect on biomass and N content of soybean (Table 1). The RDA analysis showed that soil C and N content were negatively correlated with available P content of soil (Fig. 6A). A previous study also proved that soil acidification induced by N addition decreased available P concentrations, and was associated with reductions in the relative abundance of phytase [86]. Thus, only the improvement of N nutrition in the rhizosphere microenvironment might not directly cause the plant growth promotion in available P-deficient acidic soil. Cooperation is common in nature and is a strategy conducive to community stability [87–89]. Previous studies also proved that, the bacterial community had more complex and compact associations under PGPB inoculants, the enhanced co-occurrence associations in the PGPB-inoculated bacterial network may contribute to the plant growth-promoting effects of PGPB [90], and microbial interactions may contribute to soil functions more than species diversity [91]. Thus, we believed that the addition of AMF and the enrichment of some PGPRs enhanced the stability of the rhizosphere environment and were beneficial for coping with acidic soil stress. Moreover, an increasing number of studies indicate that, in addition to complex mutual cooperation, competition may dominates the interactions among microbiome [92]. The disappearance of either cooperative party can lead to the collapse of the community, making cooperation a high-risk strategy [93].

In this study, the metabolism and absorption of N and P nutrients in plants seem to not always cause a win-win situation under environmental stress, and simply considering the enrichment/de-enrichment of certain species to evaluate the differential changes in the entire microenvironment ecology is far from enough. That's why it is necessary to consider the reconciliation roles of complex Syncoms in the rhizosphere microenvironment through multi omics techniques.

More comprehensive analysis method could lead to more stable conclusions. One significant limitation of our study was that only the composition, function and metabolism of soybean rhizosphere soil were evaluated. Whether and how the effects of Syncoms inoculation on the transcription and expression of soybean roots under stressful environments should also be examined in further studies, to better evaluate the mechanism of Syncoms regulating the rhizosphere microenvironment. Ecological fertilizer technology such as the use of Syncoms, is an important supplement to traditional synthetic chemical fertilizer technology to promote plant productivity and contribute to the abolition of hunger, but their application in ecological agriculture still needs to require extensive exploration of the complex cooperation and competition interactions in the rhizosphere microenvironment [94–96].

Conclusions

Experimental results showed that the inoculation of AMF strain *R. intraradices*, pathogenic fungus *N. oryzae* and P-solubilizing fungus *T. verruculosus* modulated the interactions among bacteria residing in the host plant niches by affecting the structure, function, and dynamics of the resident bacterial community. The inoculation of AMF *R. intraradices* improved soybean resistance to acidic soil stress by upregulating the key metabolic pathway related to plant resistance promotion under adverse environmental conditions and recruiting specific PGPR. The *N. oryzae* application stimulated the stress response in the soil microenvironment through upregulating two antibacterial activity metabolic pathways in the rhizosphere and enriching the polyene macrolide antifungal antibiotic production bacterial genus *Streptomyces* in endosphere. However, although the addition of pathogenic fungus *N. oryzae* enriched *Bradyrhizobium* and increased soil urease activity, it had no significant effect on biomass and N content of soybean. Therefore, it is necessary for us to consider the potential effect on available P content of soil when applying some microbial agents to enhance plants growth in acidic soil. Lastly, the host niches had greater impact on the assembly and shift of soybean rhizosphere microbes than the microbial agents in this short-term study. Together, our results showed that microbial agents and host niches co-mediated the fine-tuning of the compositions, functions, and metabolisms of soybean rhizosphere microbiome and further improved the survival of Al-sensitive soybean BD2 in an acidic soil. Our findings also suggested that the application of microbial agents needs to consider the complex microbe-microbe and plant-microbe interactions in specific soil environments to achieve better application effects in ecological agriculture.

Abbreviations

Al	Aluminum
C	Carbon
N	Nitrogen
P	Phosphorus
PBS	Phosphate buffered saline
AMF	Arbuscular mycorrhizal fungi
Ri	Rhizophagus intraradices
No	Nigrospora oryzae
Tv	Talaromyces verruculosus
PGPR	plant growth promoting rhizobacteria
Rh	Rhizosphere soil
Rt	Root endosphere
PCoA	Principal coordinate analysis
VIP	Variable importance of projection
GC-MS	Gas Chromatograph-Mass Spectrometer
LC-MS	Liquid Chromatograph-Mass Spectrometer

Supplementary Information

The online version contains supplementary material available at https://doi.org/10.1186/s40793-024-00624-y.

Supplementary Material 1

Supplementary Material 2

Supplementary Material 3

Supplementary Material 4

Supplementary Material 5

Supplementary Material 6

Supplementary Material 7

Supplementary Material 8

Supplementary Material 9

Acknowledgements

The authors thank the Home for Researchers (www.home-for-researchers.com) for the grammar modifications.

Author contributions

Conceptualization and Methodology: ZW, MY, and YY; Validation and Investigation: MY, ZW, YS, HM, ZL, JD, and AF; Software, Data Curation and Formal analysis: ZW, MY, AF, YS, HM, ZL, JD, TY, KN, SS, JQ and GL; Writing and Visualization: YY, ZW, MY, and AF; Supervision, Project administration and Funding acquisition: ZW, MY, and YY. All authors read and approved the final manuscript.

Funding

This work was supported by grants from the National Natural Science Foundation of China (32101383, 42377327), the China Postdoctoral Science Foundation (2023T160299, 2023M731604, 2022M711562) and the Program for Changjiang Scholars and Innovative Research Team in University from the Ministry of Education of China (IRT_14R27).

Data availability
The clean sequencing data of 16 S rRNA V3-V4 hypervariable region were uploaded to NCBI Sequence Read Archive database, and the accession number is SRP424056 (BioProject ID: PRJNA937876; reviewer link: https://dataview.ncbi.nlm.nih.gov/object/PRJNA937876?reviewer=u32bc58l2m37c9gsgaj2bia8d3). The raw data of Metabolomics were uploaded to database MetaboLights, and the project number is MTBLS7299 (link: www.ebi.ac.uk/metabolights/MTBLS7299).

Declarations

Ethics approval and consent to participate
Not applicable.

Consent for publication
Not applicable.

Competing interests
The authors declare no competing interests.

Author details
[1]State Key Laboratory of Pharmaceutical Biotechnology, Institute for Plant Molecular Biology, School of Life Sciences, Nanjing University, Nanjing 210023, China
[2]Co-Innovation Center for Sustainable Forestry in Southern China, Nanjing Forestry University, Nanjing 210037, China
[3]School of Life Sciences, Huaiyin Normal University, Huaian 223300, China

Received: 12 July 2024 / Accepted: 15 October 2024
Published online: 22 October 2024

References

1. Zhang RF, Vivanco JM, Shen QR. The unseen rhizosphere root-soil-microbe interactions for crop production. Curr Opin Microbiol. 2017;37:8–14. https://doi.org/10.1016/j.mib.2017.03.008.
2. Miki T, Ushio M, Fukui S, Kondoh M. Functional diversity of microbial decomposers facilitates plant coexistence in a plant-microbe-soil feedback model. Proc Natl Acad Sci USA. 2010;107:14251–6. https://doi.org/10.1073/pnas.0914281107.
3. Ke PJ, Miki T, Ding TS. The soil microbial community predicts the importance of plant traits in plant-soil feedback. New Phytol. 2015;206(1):329–41. https://doi.org/10.1111/nph.13215.
4. Trivedi P, Leach JE, Tringe SG, Sa T, Singh BK. Plant-microbiome interactions: from community assembly to plant health. Nat Rev Microbiol. 2020;18(1):607–21. https://doi.org/10.1038/s41579-020-0412-1.
5. Sokol NW, Slessarev E, Marschmann GL, Nicolas A, Blazewicz SJ, Brodie EL, Firestone MK, Foley MM, Hestrin R, Hungate BA, Koch BJ, Stone BW, Sullivan MB, Zablocki O, Pett-Ridge J, Consortium LSM. Life and death in the soil microbiome: how ecological processes influence biogeochemistry. Nat Rev Microbiol. 2022;20(7):415–30. https://doi.org/10.1038/s41579-022-00695-z.
6. Bulgarelli D, Garrido-Oter R, Munch PC, Weiman A, Droge J, Pan Y, McHardy AC, Schulze-Lefert P. Structure and function of the bacterial root microbiota in wild and domesticated barley. Cell Host Microbe. 2015;17(3):392–403. https://doi.org/10.1016/j.chom.2015.01.011.
7. van der Heijden MG, Bardgett RD, van Straalen NM. The unseen majority: soil microbes as drivers of plant diversity and productivity in terrestrial ecosystems. Ecol Lett. 2008;11(3):296–310. https://doi.org/10.1111/j.1461-0248.2007.01139.x.
8. Grumberg BC, Urcelay C, Shroeder MA, Vargas-Gil S, Luna CM. The role of inoculum identity in drought stress mitigation by arbuscular mycorrhizal fungi in soybean. Biol Fertil Soils. 2015;51(1):1–10. https://doi.org/10.1007/s00374-014-0942-7.
9. Evelin H, Kapoor R, Giri B. Arbuscular mycorrhizal fungi in alleviation of salt stress: a review. Ann Bot. 2009;104(7):1263–80. https://doi.org/10.1093/aob/mcp251.
10. Wang XL, Feng H, Wang YY, Wang MX, Xie XG, Chang HZ, Wang LK, Qu JC, Sun K, He W, Wang CY, Dai CC, Chu ZH, Tian CF, Yu N, Zhang XB, Liu H, Wang ET. Mycorrhizal symbiosis modulates the rhizosphere microbiota to promote rhizobia-legume symbiosis. Mol Plant. 2021;14(3):503–16. https://doi.org/10.1016/j.molp.2020.12.002.
11. de Novais CB, Sbrana C, Jesus EC, Rouws LFM, Giovannetti M, Avio L, Siqueira JO, Saggin OJ, da Silva EMR, de Faria SM. Mycorrhizal networks facilitate the colonization of legume roots by a symbiotic nitrogen-fixing bacterium. Mycorrhiza. 2020;30(2–3):389–96. https://doi.org/10.1007/s00572-020-00948-w.
12. Igiehon NO, Babalola OO, Cheseto X, Torto B. Effects of rhizobia and arbuscular mycorrhizal fungi on yield, size distribution and fatty acid of soybean seeds grown under drought stress. Microbiol Res. 2021;242:126640. https://doi.org/10.1016/j.micres.2020.126640.
13. Xie XG, Zhang FM, Yang T, Chen Y, Li XG, Dai CC. Endophytic fungus drives nodulation and N_2 fixation attributable to specific root exudates. mBio. 2019;10(4):e00728–19. https://doi.org/10.1128/mBio.00728-19.
14. Zhang JE, Feng LF, Ouyang Y, Hu RR, Xu HQ, Wang JX. Phosphate-solubilizing bacteria and fungi in relation to phosphorus availability under different land uses for some latosols from Guangdong, China. CATENA. 2020;195:104686. https://doi.org/10.1016/j.catena.2020.104686.
15. Wu JR, Xu FJ, Cao W, Zhang W, Guan YX, Dai CC. Fungal endophyte *Phomopsis Liquidambari* B3 enriches the diversity of nodular culturable endophytic bacteria associated with continuous cropping of peanut. Arch Agron Soil Sci. 2019;65(2):240–52. https://doi.org/10.1080/03650340.2018.1493198.
16. Zhang W, Li XG, Sun K, Tang MJ, Xu FJ, Zhang M, Dai CC. Mycelial network-mediated rhizobial dispersal enhances legume nodulation. ISME J. 2020;14(4):1015–29. https://doi.org/10.1038/s41396-020-0587-5.
17. Trivedi P, Trivedi C, Grinyer J, Anderson IC, Singh BK. Harnessing host-vector microbiome for sustainable plant disease management of phloem-limited bacteria. Front Plant Sci. 2016;7:1423. https://doi.org/10.3389/fpls.2016.01423.
18. Zhang C, van der Heijden MGA, Dodds BK, Nguyen TB, Spooren J, Valzano-Held A, Cosme M, Berendsen RL. A tripartite bacterial-fungal-plant symbiosis in the mycorrhiza-shaped microbiome drives plant growth and mycorrhization. Microbiome. 2024;12(1):13. https://doi.org/10.1186/s40168-023-01726-4.
19. Hestrin R, Hammer EC, Mueller CW, Lehmann J. Synergies between mycorrhizal fungi and soil microbial communities increase plant nitrogen acquisition. Commun Biol. 2019;2(1):233. https://doi.org/10.1038/s42003-019-0481-8.
20. Trivedi P, Leach JE, Tringe SG, Sa T, Singh BK. Plant-microbiome interactions: from community assembly to plant health. Nat Rev Microbiol. 2020;18:607–21. https://doi.org/10.1038/s41579-020-0412-1.
21. Vonuexkull HR, Mutert E. Global extent, development and economic-impact of acid soils. Plant Soil. 1995;171(1):1–15. https://doi.org/10.1007/BF00009558.
22. Ryan PR, Shaff JE, Kochian LV. Aluminum toxicity in roots - correlation among ionic currents, ion fluxes, and root elongation in aluminum-sensitive and aluminum-tolerant wheat cultivars. Plant Physiol. 1992;99(3):1193–200. https://doi.org/10.1104/pp.99.3.1193.
23. Farh MEA, Kim YJ, Sukweenadhi J, Singh P, Yang DC. Aluminium resistant, plant growth promoting bacteria induce overexpression of aluminium stress related genes in *Arabidopsis thaliana* and increase the ginseng tolerance against aluminium stress. Microbiol Res. 2017;200:45–52. https://doi.org/10.1016/j.micres.2017.04.004.
24. Raza S, Miao N, Wang PZ, Ju XT, Chen ZJ, Zhou JB, Kuzyakov Y. Dramatic loss of inorganic carbon by nitrogen-induced soil acidification in Chinese croplands. Glob Chang Biol. 2020;26(6):3738–51. https://doi.org/10.1111/gcb.15101.
25. Huang SC, Chu SJ, Guo YM, Ji YJ, Hu DQ, Cheng J, Lu GH, Yang RW, Tang CY, Qi JL, Yang YH. Novel mechanisms for organic acid-mediated aluminium tolerance in roots and leaves of two contrasting soybean genotypes. AoB Plants. 2017;9:plx064. https://doi.org/10.1093/aobpla/plx064.
26. Wen ZL, Yang MK, Fazal A, Han HH, Lin HY, Yin TM, Zhu YL, Yang SP, Niu KC, Sun SC, Qi JL, Lu GH, Yang YH. Harnessing the power of microbes: enhancing soybean growth in an acidic soil through AMF inoculation rather than P-fertilization. Hortic Res. 2024;11:uhae067. https://doi.org/10.1093/hr/uhae067.
27. Yang TY, Liu GL, Li YC, Zhu SM, Zou AL, Qi JL, Yang YH. Rhizosphere microbial communities and organic acids secreted by aluminum-tolerant and aluminum-sensitive soybean in acid soil. Biol Fert Soils. 2012;48(1):97–108. https://doi.org/10.1007/s00374-011-0608-7.
28. Zhang S, Zhou J, Wang GH, Wang XR, Liao H. The role of mycorrhizal symbiosis in aluminum and phosphorus interactions in relation to aluminum tolerance in soybean. Appl Microbiol Biotechnol. 2015;99(23):10225–35. https://doi.org/10.1007/s00253-015-6913-6.
29. Seguel A, Cumming JR, Klugh-Stewart K, Cornejo P, Borie F. The role of arbuscular mycorrhizas in decreasing aluminium phytotoxicity in acidic

soils: a review. Mycorrhiza. 2013;23(3):167–83. https://doi.org/10.1007/s00572-013-0479-x.
30. Lin MH, Gresshoff PM, Ferguson BJ. Systemic regulation of soybean nodulation by acidic growth conditions. Plant Physiol. 2012;160(4):2028–39. https://doi.org/10.1104/pp.112.204149.
31. Kunito T, Isomura I, Sumi H, Park HD, Toda H, Otsuka S, Nagaoka K, Saeki K, Senoo K. Aluminum and acidity suppress microbial activity and biomass in acidic forest soils. Soil Biol Biochem. 2016;97:23–30. https://doi.org/10.1016/j.soilbio.2016.02.019.
32. Abberton M, Batley J, Bentley A, Bryant J, Cai HW, Cockram J, Costa de Oliveira A, Cseke LJ, Dempewolf H, De Pace C, Edwards D, Gepts P, Greenland A, Hall AE, Henry R, Hori K, Howe GT, Hughes S, Humphreys M, Lightfoot D, Marshall A, Mayes S, Nguyen HT, Ogbonnaya FC, Ortiz R, Paterson AH, Tuberosa R, Valliyodan B, Varshney RK, Yano M. Global agricultural intensification during climate change: a role for genomics. Plant Biotechnol J. 2016;14(4):1095–8. https://doi.org/10.1111/pbi.12467.
33. Hickey JM, Dreisigacker S, Crossa J, Hearne S, Babu R, Prasanna BM, Grondona M, Zambelli A, Windhausen VS, Mathews K, Gorjanc G. Evaluation of genomic selection training population designs and genotyping strategies in plant breeding programs using simulation. Crop Sci. 2014;54(4):1476–88. https://doi.org/10.2135/cropsci2013.03.0195.
34. Singh JS, Pandey VC, Singh DP. Efficient soil microorganisms: a new dimension for sustainable agriculture and environmental development. Agric Ecosyst Environ. 2011;140(3–4):339–53. https://doi.org/10.1016/j.agee.2011.01.01.
35. Baum C, El-Tohamy W, Gruda N. Increasing the productivity and product quality of vegetable crops using arbuscular mycorrhizal fungi: a review. Sci Hortic. 2015;187:131–41. https://doi.org/10.1016/j.scienta.2015.03.002.
36. Olanrewaju OS, Babalola OO. Streptomyces: implications and interactions in plant growth promotion. Appl Microbiol Biotechnol. 2019;103(3):1179–88. https://doi.org/10.1007/s00253-018-09577-y.
37. Wang CH, Li YJ, Li MJ, Zhang KF, Ma WJ, Zheng L, Xu HY, Cui BF, Liu R, Yang YQ, Zhong YJ, Liao H. Functional assembly of root-associated microbial consortia improves nutrient efficiency and yield in soybean. J Integr Plant Biol. 2021;63(6):1021–35. https://doi.org/10.1111/jipb.13073.
38. Han Q, Ma Q, Chen Y, Tian B, Xu LX, Bai Y, Chen WF, Li X. Variation in rhizosphere microbial communities and its association with the symbiotic efficiency of rhizobia in soybean. ISME J. 2020;14(8):1915–28. https://doi.org/10.1038/s41396-020-0648-9.
39. Liu LR, Cheng L, Liu K, Liu Q, Gong ZH, Cai ZD, Liu JJ, Zhao XQ, Nian H, Ma QB, Lian TX. Transgenic soybean of *GsMYB10* shapes rhizosphere microbes to promote resistance to aluminum (Al) toxicity. J Hazard Mater. 2023;455:131621. https://doi.org/10.1016/j.jhazmat.2023.131621.
40. Wen ZL, Yang MK, Han HW, Fazal A, Liao YH, Ren R, Yin TM, Qi JL, Sun SC, Lu GH, Hu SJ, Yang YH. Mycorrhizae enhance soybean plant growth and aluminum stress tolerance by shaping the microbiome assembly in an acidic soil. Microbiol Spectr. 2023;11(2):e03310–22. https://doi.org/10.1128/spectrum.03310-22.
41. Zeng QP, Dong JW, Lin XR, Zhou XF, Xu HW. Isolation and identification of *Acer Truncatum* endophytic fungus *Talaromyces Verruculosus* and evaluation of its effects on insoluble phosphorus absorption capacity and growth of cucumber seedlings. J Fungi. 2024;10(2):136. https://doi.org/10.3390/jof10020136.
42. Lee H, Cho BK, Kim MS, Lee WH, Tewari J, Bae H, Sohn SI, Chi HY. Prediction of crude protein and oil content of soybeans using Raman spectroscopy. Sens Actuators B Chem. 2013;185:694–700. https://doi.org/10.1016/j.snb.2013.04.103.
43. Kennedy K, Hall MW, Lynch MDJ, Moreno-Hagelsieb G, Neufeld JD. Evaluating bias of Illumina-based bacterial 16S rRNA gene profiles. Appl Environ Microbiol. 2014;80(18):5717–22. https://doi.org/10.1128/AEM.01451-14.
44. Fadrosh DW, Ma B, Gajer P, Sengamalay N, Ott S, Brotman RM, Ravel J. An improved dual-indexing approach for multiplexed 16S rRNA gene sequencing on the Illumina MiSeq platform. Microbiome. 2014;2:6. https://doi.org/10.1186/2049-2618-2-6.
45. Bolger AM, Lohse M, Usadel B. Trimmomatic: a flexible trimmer for Illumina sequence data. Bioinformatics. 2014;30(15):2114–20. https://doi.org/10.1093/bioinformatics/btu170.
46. Magoc T, Salzberg SL. FLASH: fast length adjustment of short reads to improve genome assemblies. Bioinformatics. 2011;27(21):2957–63. https://doi.org/10.1093/bioinformatics/btr507.
47. Caporaso JG, Kuczynski J, Stombaugh J, Bittinger K, Bushman FD, Costello EK, Fierer N, Peña AG, Goodrich JK, Gordon JI, et al. QIIME allows analysis of high-throughput community sequencing data. Nat Methods. 2010;7(5):335–6. https://doi.org/10.1038/nmeth.f.303.
48. Edgar RC, Haas BJ, Clemente JC, Quince C, Knight R. UCHIME improves sensitivity and speed of chimera detection. Bioinformatics. 2011;27(16):2194–200. https://doi.org/10.1093/bioinformatics/btr381.
49. Rognes T, Flouri T, Nichols B, Quince C, Mahé F. VSEARCH: a versatile open source tool for metagenomics. PeerJ. 2016;4:e2584. https://doi.org/10.7717/peerj.2584.
50. Caporaso JG, Kuczynski J, Stombaugh J, Bittinger K, Bushman FD, Costello EK, Fierer N, Pena AG, Goodrich JK, Gordon JI, Huttley GA, Kelley ST, Knights D, Koenig JE, Ley RE, Lozupone CA, McDonald D, Muegge BD, Pirrung M, Reeder J, Sevinsky JR, Tumbaugh PJ, Walters WA, Widmann J, Yatsunenko T, Zaneveld J, Knight R. QIIME allows analysis of high-throughput community sequencing data. Nat Methods. 2010;7(5):335–6. https://doi.org/10.1038/nmeth.f.303.
51. Schloss PD, Westcott SL, Ryabin T, Hall JR, Hartmann M, Hollister EB, Lesniewski RA, Oakley BB, Parks DH, Robinson CJ, Sahl JW, Stres B, Thallinger GG, Van Horn DJ, Weber CF. Introducing mothur: open-source, platform-independent, community-supported software for describing and comparing microbial communities. Appl Environ Microbiol. 2009;75(23):7537–41. https://doi.org/10.1128/AEM.01541-09.
52. Zhao LJ, Zhang HL, White JC, Chen XQ, Li HB, Qu XL, Ji R. Metabolomics reveals that engineered nanomaterial exposure in soil alters both soil rhizosphere metabolite profiles and maize metabolic pathways. Environ Sci Nano. 2019;6(6):1716–27. https://doi.org/10.1039/c9en00137a.
53. Fu Q, Lai JL, Ji XH, Luo ZX, Wu G, Luo XG. Alterations of the rhizosphere soil microbial community composition and metabolite profiles of *Zea mays* by polyethylene-particles of different molecular weights. J Hazard Mater. 2022;423:127062. https://doi.org/10.1016/j.jhazmat.2021.127062.
54. Zhang HY, Liu SR, Qin QZ, Xu ZH, Qu Y, Wang YD, Wang JN, Du ZZ, Yuan SS, Hong SM, Chang ZL, He WY, Yan XL, Lang YR, Tang RY, Wang Y, Zhu LL, Jiang XX. Genetic and pharmacological inhibition of astrocytic mysm1 alleviates depressive-like disorders by promoting ATP production. Adv Sci. 2022;10(1):e2204463. https://doi.org/10.1002/advs.202204463.
55. Lai JL, Deng ZX, Ji XH, Luo XG. Absorption and interaction mechanisms of uranium & cadmium in purple sweet potato (*Ipomoea batatas* L). J Hazard Mater. 2020;400:123264. https://doi.org/10.1016/j.jhazmat.2020.123264.
56. Yang X, Lai JL, Zhang Y, Luo XG, Han MW, Zhao SP. Microbial community structure and metabolome profiling characteristics of soil contaminated by TNT, RDX, and HMX. Environ Pollut. 2021;285:117478. https://doi.org/10.1016/j.envpol.2021.117478.
57. Haug K, Cochrane K, Nainala VC, Williams M, Chang JK, Jayaseelan KV, O'Donovan C. MetaboLights: a resource evolving in response to the needs of its scientific community. Nucleic Acids Res. 2020;48(D1):D440–4. https://doi.org/10.1093/nar/gkz1019.
58. Fazal A, Yang MK, Wang X, Lu YT, Yao WX, Luo FH, Han M, Song YC, Cai JF, Yin TM, Niu KC, Sun SC, Qi JL, Lu GH, Wen ZL, Yang YH. Discrepancies in rhizobacterial assembly caused by glyphosate application and herbicide-tolerant soybean co-expressing *GAT* and *EPSPS*. J Hazard Mater. 2023;450:131053. https://doi.org/10.1016/j.jhazmat.2023.131053.
59. Zhou JZ, Wu LY, Deng Y, Zhi XY, Jiang YH, Tu QC, Xie JP, Van Nostrand JD, He ZL, Yang YF. Reproducibility and quantitation of amplicon sequencing-based detection. ISME J. 2011;5(8):1303–13. https://doi.org/10.1038/ismej.2011.11.
60. Zhang HL, Lu L, Zhao XP, Zhao S, Gu XY, Du WC, Wei H, Ji R, Zhao LJ. Metabolomics reveals the invisible responses of spinach plants exposed to CeO_2 nanoparticles. Environ Sci Technol. 2019;53(10):6007–17. https://doi.org/10.1021/acs.est.9b00593.
61. Shayanthan A, Ordoñez PAC, Oresnik IJ. The role of Synthetic Microbial communities (SynCom) in sustainable agriculture. Front Agron. 2022;4:896307. https://doi.org/10.3389/fagro.2022.896307.
62. Xun W, Liu Y, Ma A, Yan H, Miao Y, Shao J, Zhang N, Xu Z, Shen Q, Zhang R. Dissection of rhizosphere microbiome and exploiting strategies for sustainable agriculture. New Phytol. 2024;242(6):2401–10. https://doi.org/10.1111/nph.19697.
63. Goyari S, Devi SH, Bengyella L, Khan M, Sharma CK, Kalita MC, Talukdar NC. Unveiling the optimal parameters for cellulolytic characteristics of *Talaromyces Verruculosus* SGMNPf3 and its secretory enzymes. J Appl Microbiol. 2015;119(1):88–98. https://doi.org/10.1111/jam.12816.
64. Sharma A, Shankhdhar D, Sharma A, Shankhdhar SC. Growth promotion of the rice genotypes by pgprs isolated from rice rhizosphere. J Soil Sci Plant Nutr. 2014;14(2):505–17. https://doi.org/10.4067/S0718-95162014005000040.
65. Su P, Kang HX, Peng QZ, Wicaksono WA, Berg G, Liu ZX, Ma JJ, Zhang DY, Cernava T, Liu Y. 2024. Microbiome homeostasis on rice leaves is regulated

by a precursor molecule of lignin biosynthesis. Nat Commun. 2024;15(1):23. https://doi.org/10.1038/s41467-023-44335-3
66. Gai X, Xing WL, Chen GC. Divergent responses of rhizosphere soil phosphorus fractions and biological features of *Salix psammophila* to fertilization strategies under cadmium contamination. Sci Total Environ. 2024;929:172554. https://doi.org/10.1016/j.scitotenv.2024.172554.
67. Kim JD, Kang JE, Kim BS. Postharvest disease control efficacy of the polyene macrolide lucensomycin produced by *Streptomyces plumbeus* strain CA5 against gray mold on grapes. Postharvest Biol Tec. 2020;162:111115. https://doi.org/10.1016/j.postharvbio.2019.111115.
68. Aparicio JF, Barreales EG, Payero T, Vicente CM, de Pedro A, Santos-Aberturas J. Biotechnological production and application of the antibiotic pimaricin: biosynthesis and its regulation. Appl Microbiol Biotechnol. 2016;100(1):61–78. https://doi.org/10.1007/s00253-015-7077-0.
69. Jin Z, Jiang F, Wang L, Declerck S, Feng G, Zhang L. Arbuscular mycorrhizal fungi and *Streptomyces*: brothers in arms to shape the structure and function of the hyphosphere microbiome in the early stage of interaction. Microbiome. 2024;12(1):83. https://doi.org/10.1186/s40168-024-01811-2.
70. Wang BY, Xiao QC, Geng XW, Lin KQ, Li ZS, Li YY, Chen J, Li XY. Arbuscular mycorrhizal fungi alter rhizosphere bacterial diversity, network stability and function of lettuce in barren soil. Sci Hortic. 2024;323:112533. https://doi.org/10.1016/j.scienta.2023.112533.
71. Wang HR, Du XR, Zhang ZY, Feng FJ, Zhang JM. Rhizosphere interface microbiome reassembly by arbuscular mycorrhizal fungi weakens cadmium migration dynamics. iMeta. 2023;2(4):e133. https://doi.org/10.1002/imt2.133.
72. Hoang DTT, Rashtbari M, Anh LT, Wang S, Tu DT, Hiep NV, Razavi BS. Mutualistic interaction between arbuscular mycorrhiza fungi and soybean roots enhances drought resistant through regulating glucose exudation and rhizosphere expansion. Soil Biol Biochem. 2022;171:108728. https://doi.org/10.1016/j.soilbio.2022.108728.
73. Sasse J, Martinoia E, Northen T. Feed your friends: do plant exudates shape the root microbiome? Trends Plant Sci. 2018;23(1):25–41. https://doi.org/10.1016/j.tplants.2017.09.003.
74. Kong ZY, Liu HG. Modification of rhizosphere microbial communities: a possible mechanism of plant growth promoting rhizobacteria enhancing plant growth and fitness. Front Plant Sci. 2022;13:920813. https://doi.org/10.3389/fpls.2022.920813.
75. Li YZ, Xu LN, Letuma P, Lin WX. Metabolite profiling of rhizosphere soil of different allelopathic potential rice accessions. BMC Plant Biol. 2020;20(1):265. https://doi.org/10.1186/s12870-020-02465-6.
76. Saeidi M, Raei Y, Amini R, Taghizadeh A, Pasban-Eslam B. Changes in fatty acid and protein of safflower as response to biofertilizers and cropping system. Turk J Field Crops. 2018;23(2):117–26. https://doi.org/10.17557/tjfc.471666.
77. Mei CS, Zhou DF, Chretien RL, Turner A, Hou GC, Evans MR, Lowman S. A potential application of *Pseudomonas psychrotolerans* IALR632 for lettuce growth promotion in hydroponics. Microorganisms. 2023;11(2):376. https://doi.org/10.3390/microorganisms11020376.
78. Zheng Y, Cao X, Zhou Y, Ma S, Wang Y, Li Z, Zhao D, Yang Y, Zhang H, Meng C, Xie Z, Sui X, Xu K, Li Y, Zhang CS. Purines enrich root-associated *Pseudomonas* and improve wild soybean growth under salt stress. Nat Commun. 2024;15(1):3520. https://doi.org/10.1038/s41467-024-47773-9.
79. Wang ZH, Song Y. Toward understanding the genetic bases underlying plant-mediated cry for help to the microbiota. iMeta. 2022;1(1):e8. https://doi.org/10.1002/imt2.8.
80. Nolan TM, Vukasinovic N, Liu DR, Russinova E, Yin YH, Brassinosteroids. Multidimensional regulators of plant growth, development, and stress responses. Plant Cell. 2020;32(2):295–318. https://doi.org/10.1105/tpc.19.00335.
81. Fan YT, Shen JL, Liu XL, Cui JH, Liu JY, Peng DQ, Jin YC. β-sitosterol suppresses lipopolysaccharide-induced inflammation and lipogenesis disorder in bovine mammary epithelial cells. Int J Mol Sci. 2023;24(19):14644. https://doi.org/10.3390/ijms241914644.
82. Rashid PT, Hossain MJ, Zahan MS, Hasan CM, Rashid MA, Al-Mansur MA, Haque MR. Chemico-pharmacological and computational studies of *Ophiorrhiza Fasciculata* D. Don and *Psychotria silhetensis* hook. f. focusing cytotoxic, thrombolytic, anti-inflammatory, antioxidant, and antibacterial properties. Heliyon. 2023;9(9):e20100. https://doi.org/10.1016/j.heliyon.2023.e20100.
83. Ezak MJ, Hong E, Chaparro-Garcia A, Ferkey DM. *Caenorhabditis elegans* TRPV channels function in a modality-specific pathway to regulate response to aberrant sensory signaling. Genetics;2010, 185(1):233-U357. https://doi.org/10.1534/genetics.110.115188
84. Gharbi H, Fabretti F, Bharill P, Rinschen MM, Brinkkötter S, Frommolt P, Burst V, Schermer B, Benzing T, Müller RU. Loss of the birt-hogg-dube gene product folliculin induces longevity in a hypoxia-inducible factor-dependent manner. Aging Cell. 2013;12(4):593–603. https://doi.org/10.1111/acel.12081.
85. Wang L, Luo XS, Xiong X, Chen WL, Hao XL, Huang QY. Soil aggregate stratification of ureolytic microbiota affects urease activity in an inceptisol. J Agr Food Chem. 2019;67(42):11584–90. https://doi.org/10.1021/acs.jafc.9b04244.
86. Tian J, Dungait JAJ, Lu XK, Yang YF, Hartley IP, Zhang W, Mo JM, Yu GR, Zhou JZ, Kuzyakov Y. Long-term nitrogen addition modifies microbial composition and functions for slow carbon cycling and increased sequestration in tropical forest soil. Glob Chang Biol. 2019;25(10):3267–81. https://doi.org/10.1111/gcb.14750.
87. Giri S, Yousif G, Shitut S, Ona L, Kost C. Prevalent emergence of reciprocity among cross-feeding bacteria. ISME Commun. 2022;2(1):71. https://doi.org/10.1038/s43705-022-00155-y.
88. Giri S, Ona L, Waschina S, Shitut S, Yousif G, Kaleta C, Kost C. Metabolic dissimilarity determines the establishment of cross-feeding interactions in bacteria. Curr Biol. 2021;31(24):5547–e55575546. https://doi.org/10.1016/j.cub.2021.10.019.
89. Ona L, Kost C. Cooperation increases robustness to ecological disturbance in microbial cross-feeding networks. Ecol Lett. 2022;25(6):1410–20. https://doi.org/10.1111/ele.14006.
90. Kong ZY, Wu ZJ, Glick BR, He SY, Huang C, Wu L. Co-occurrence patterns of microbial communities affected by inoculants of plant growth-promoting bacteria during phytoremediation of heavy metal contaminated soils. Ecotox Environ Safe. 2019;183:109504. https://doi.org/10.1016/j.ecoenv.2019.109504.
91. Ma B, Wang HZ, Dsouza M, Lou J, He Y, Dai ZM, Brookes PC, Xu JM, Gilbert JA. Geographic patterns of co-occurrence network topological features for soil microbiota at continental scale in eastern China. ISME J. 2016;10(8):1891–901. https://doi.org/10.1038/ismej.2015.261.
92. Coyte KZ, Schluter J, Foster KR. The ecology of the microbiome: networks, competition, and stability. Science. 2015;350(6261):663–6. https://doi.org/10.1126/science.aad2602.
93. Oliveira NM, Niehus R, Foster KR. Evolutionary limits to cooperation in microbial communities. Proc Natl Acad Sci USA. 2014;111(50):17941–6. https://doi.org/10.1073/pnas.1412673111.
94. Hu HW, Chen QL, He JZ. The end of hunger: fertilizers, microbes and plant productivity. Microb Biotechnol. 2022;15(4):1050–4. https://doi.org/10.1111/1751-7915.13973.
95. Batista BD, Singh BK. Realities and hopes in the application of microbial tools in agriculture. Microb Biotechnol. 2021;14(4):1258–68. https://doi.org/10.1111/1751-7915.13866.
96. Vorholt JA, Vogel C, Carlstrom CI, Muller DB. Establishing causality: opportunities of synthetic communities for plant microbiome research. Cell Host Microbe. 2017;22(2):142–55. https://doi.org/10.1016/j.chom.2017.07.004.

Publisher's note